



Energy release patterns and shaking effects of earthquakes in the Japan Trench: A Hilbert-Huang Transform approach

Swapnil Mache and Kusala Rajendran

Indian Institute of Science (IISc), Bangalore, India



1. Key Points

- 1. Specific Intrinsic Mode Functions (IMFs) represent energy release at the earthquake source.
- 2. Energy Rate Functions (ERFs) generated from Hilbert spectral analysis of such IMF combinations.
- 3. Proposed ERFs match well with the Moment Rate Functions (MRFs) from teleseismic waveform modeling.
- 4. ERF-MRF match is controlled by the station azimuth and shaking intensity, and frequency and energy-based selection of IMFs.

A short video explaining our work:

2. Motivation

- 1. Subduction zone earthquakes showcase different energy release patterns and frequency content depending on the **tectonic setting and depth**.
- 2. Interplate earthquakes, originating on the plate interface, show enhanced high-frequency energy (HFE) with increasing depth (Lay et al., 2012).
- 3. Outer-rise intraplate earthquakes produce enhanced HFE and ground shaking despite their high epicentral distances (Ye et al., 2013).
- 4. Intraslab earthquakes originate within the subduction slab (usually beneath population centers). They are more damaging than other similar Mw events due to enhanced HFE release and associated ground motion in a short duration, along with higher stress

3. Data

- 1. **Teleseismic data** from International Research Institutions for Seismology (IRIS). P and SH waveforms from 30-40 stations, epicentral distance 30° to 90°.
- 2. **Strong-motion acceleration data** from KiK-net, National Research Institute for Earth Science and Disaster Resilience (NIED, Japan). Data from the **vertical component of borehole sensors** (> 100 m depth) used in the analysis.

Event Number	Event Date (YYYY-MM-DD)	Event Time (hh:mm:ss.s)	Longitude (°E)	Latitude (°N)	Depth (km)	Mw	Tectonic Setting
1	2003-05-26	09:24:38.8	141.57	38.94	61.0	7.0	Intraslab
2	2011-04-07	14:32:50.6	141.85	38.32	53.3	7.1	Intraslab
3	2005-08-16	02:46:40.3	142.05	38.24	37.0	7.5	Interplate
4	2006-07-19	02:39:34.5	142.42	37.47	21.5	6.9	Interplate
5	2012-12-07	08:18:34.9	144.09	38.01	57.8	7.2	Intraplate
		08:18:46.9	143.83	37.77	19.5	7.2	Intraplate

Table: Earthquake details (from GCMT).

4. Methodology

Waveform inversion of teleseismic data

- 1. Kikuchi-Kanamori body-wave inversion program (Kikuchi and Kanamori, 1991) used for the analysis.
- 2. Moment Rate Function (MRF) generated from waveform modeling to validate the ERF algorithm.

Selection of strong-motion stations

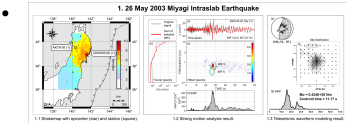
- 1. Slip distribution, along with the seismic intensity distribution maps (JMA, 1996; ShakeMap, 2017), used to select stations within the inferred azimuthal range and seismic intensity > 3.



5. Results

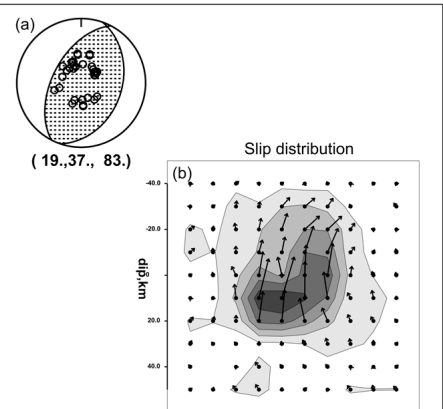
1. 26 May 2003 Miyagi Intraslab Earthquake (Mw 7.0, depth 67.0 km)

- Up-dip slip (towards east-northeast).
- Station AKTH16, WNW (305.98° azimuth), seismic intensity (SI) 4.
- Single, dominant, ~10 s energy pulse captured by both the ERF and MRF, along with a weaker tail.

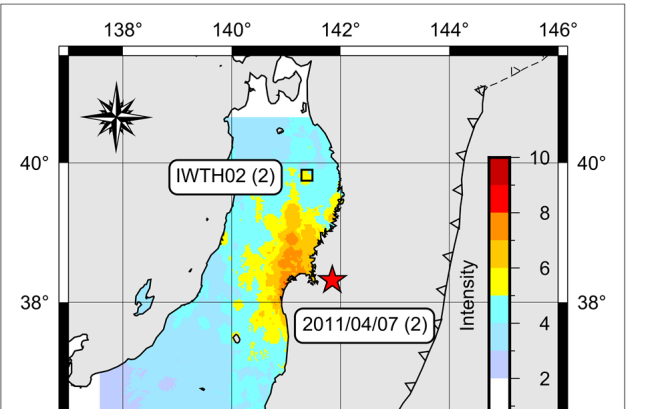


2. 07 April 2011 Miyagi Intraslab

Waveform Modeling



Strong motion station selection



6. Summary

- 1. HHT-based **ERF captures the earthquake source energy release**, with a **higher resolution** offered by HHT as compared to Fourier analysis methods and wavelet transform.
- 2. **ERF retains frequency information**, is computationally faster for a rapid interpretation of an event, and **does not entail assumptions** of the fault geometry and velocity structure. These are clear advantages over the traditional MRF.
- 3. **ERF captures complex ruptures** (2005 Miyagi-Oki event) and sub-events or multiple independent events (2012 Kamaishi event).

1. Key Points

1. Specific Intrinsic Mode Functions (IMFs) represent energy release at the earthquake source.
2. Energy Rate Functions (ERFs) generated from Hilbert spectral analysis of such IMF combinations.
3. Proposed ERFs match well with the Moment Rate Functions (MRFs) from teleseismic waveform modeling.
4. ERF-MRF match is controlled by the station azimuth and shaking intensity, and frequency and energy-based selection of IMFs.

A short video explaining our work:

4. Methodology

Waveform inversion of teleseismic data

1. Kikuchi-Kanamori body-wave inversion program (Kikuchi and Kanamori, 1991) used for the analysis.
2. Moment Rate Function (MRF) generated from waveform modeling to validate the ERF algorithm.

Selection of strong-motion stations

1. Slip distribution, along with the seismic intensity distribution maps (JMA, 1996; ShakeMap, 2017), used to select stations within the inferred azimuthal range and seismic intensity > 3.

6. Summary

1. HHT-based ERF captures the earthquake source energy release, with a **higher resolution** offered by HHT as compared to Fourier analysis methods and wavelet transform.
2. ERF retains frequency information, is computationally faster for a rapid interpretation of an event, and **does not entail assumptions** of the fault geometry and velocity structure. These are clear advantages over the traditional MRF.
3. ERF captures complex ruptures (2005 Miyagi-Oki event) and sub-events or

2. Motivation

1. Subduction zone earthquakes showcase different energy release patterns and frequency content depending on the **tectonic setting and depth**.
2. Interplate earthquakes, originating on the plate interface, show enhanced high-frequency energy (HFE) with increasing depth (Lay et al., 2012).
3. Outer-rise intraplate earthquakes produce enhanced HFE and ground shaking despite their high epicentral distances (Ye et al., 2013).
4. Intraslab earthquakes originate within the subduction slab (usually beneath population centers). They are more damaging than other similar Mw events due to enhanced HFE release and associated ground motion in a short duration, along with higher stress drop, increasing with depth (Choy et al., 2001; Okal and Kirby, 2002).
5. Conventional time-frequency analysis methods (Fourier transform, short-time Fourier transform, continuous wavelet transform) are deficient in resolving the above properties. They have a priori defined bases, are not suitable for nonlinear and nonstationary earthquake signals, and have limited resolution (Huang et al., 1998; Tary et al., 2014).
6. **Hilbert-Huang Transform (HHT)** overcomes these drawbacks

Energy release pa



Key Points

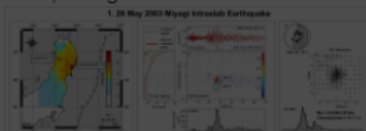
Specific Intrinsic Mode Functions (IMFs) represent energy release at the earthquake source. Energy Rate Functions (ERFs) generated from Hilbert spectral analysis of such IMF combinations. Proposed ERFs match well with the Moment Rate Functions (MRFs) from teleseismic waveform modeling. ERF-MRF match is controlled by the station azimuth and shaking intensity, and frequency and energy-based selection of IMFs.

Short video explaining our work

OPEN

Results

- 26 May 2003 Miyagi Intraslab Earthquake (Mw 7.0, depth 67.0 km)**
- Up-dip slip (towards east-northeast).
 - Station AKTH16, WNW (305.98° azimuth), seismic intensity (SI) 4.
 - Single, dominant, ~10 s energy pulse captured by both the ERF and MRF, along with a weaker tail.



n: A Hilbert-Huang



4. Methodology

Waveform inversion of teleseismic data

1. Kikuchi-Kanamori body-wave inversion program (Kikuchi and Kanamori, 1991) used for the analysis.
2. Moment Rate Function (MRF) generated from waveform modeling to validate the ERF algorithm.

Selection of strong-motion stations

1. Slip distribution, along with the seismic intensity distribution maps (JMA, 1996; ShakeMap, 2017), used to select stations within the inferred azimuthal range and seismic intensity > 3.

OPEN

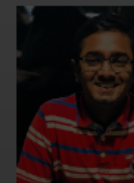
6. Summary

1. HHT-based **ERF captures the earthquake source energy release**, with a **higher resolution** offered by HHT as compared to Fourier analysis methods and wavelet transform.
2. **ERF retains frequency information**, is computationally faster for a rapid interpretation of an event, and **does not entail assumptions** of the fault geometry and velocity structure. These are clear advantages over the traditional MRF.
3. **ERF captures complex ruptures** (2005 Miyagi-Oki event) and sub-events or

2. Motivation

2. Interplate earthquakes, originating on the plate interface, show enhanced high-frequency energy (HFE) with increasing depth (Lay et al., 2012).
3. Outer-rise intraplate earthquakes produce enhanced HFE and ground shaking despite their high epicentral distances (Ye et al., 2013).
4. Intraslab earthquakes originate within the subduction slab (usually beneath population centers). They are more damaging than other similar Mw events due to enhanced HFE release and associated ground motion in a short duration, along with higher stress drop, increasing with depth (Choy et al., 2001; Okal and Kirby, 2002).
5. Conventional time-frequency analysis methods (Fourier transform, short-time Fourier transform, continuous wavelet transform) are deficient in resolving the above properties. They have a priori defined bases, are not suitable for nonlinear and nonstationary earthquake signals, and have limited resolution (Huang et al., 1998; Tary et al., 2014).
6. **Hilbert-Huang Transform (HHT)** overcomes these drawbacks and provides instantaneous frequency and energy, which we leverage to analyze energy release from five earthquakes, originating in different tectonic settings and depths.

n: A Hilbert-Huang



4. Methodology

Waveform inversion of teleseismic data

1. Kikuchi-Kanamori body-wave inversion program (Kikuchi and Kanamori, 1991) used for the analysis.
2. Moment Rate Function (MRF) generated from waveform modeling to validate the ERF algorithm.

Selection of strong-motion stations

1. Slip distribution, along with the seismic intensity distribution maps (JMA, 1996; ShakeMap, 2017), used to select stations within the inferred azimuthal range and seismic intensity > 3.

OPEN

6. Summary

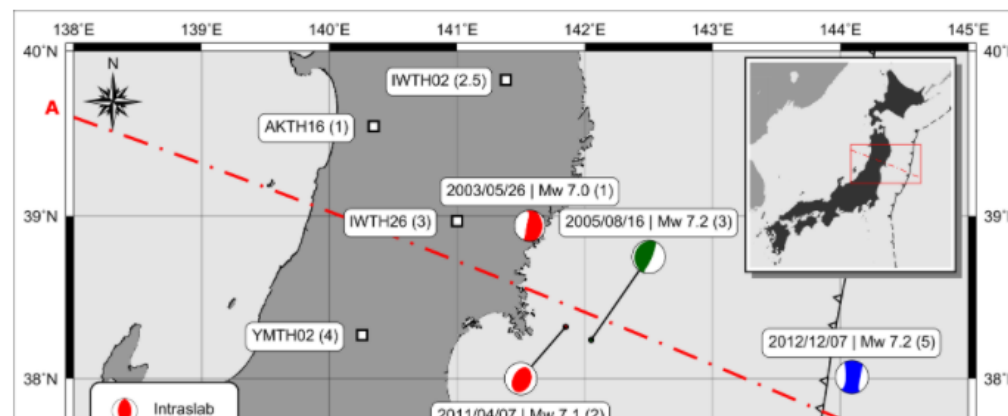
1. HHT-based **ERF captures the earthquake source energy release**, with a **higher resolution** offered by HHT as compared to Fourier analysis methods and wavelet transform.
2. **ERF retains frequency information**, is computationally faster for a rapid interpretation of an event, and **does not entail assumptions** of the fault geometry and velocity structure. These are clear advantages over the traditional MRF.
3. **ERF captures complex ruptures** (2005 Miyagi-Oki event) and sub-events or

3. Data

1. **Teleseismic data** from International Research Institutions for Seismology (IRIS). P and SH waveforms from 30-40 stations, epicentral distance 30° to 90° .
2. **Strong-motion acceleration data** from KiK-net, National Research Institute for Earth Science and Disaster Resilience (NIED, Japan). Data from the **vertical component of borehole sensors** (> 100 m depth) used in the analysis.

Event Number	Event Date (YYYY-MM-DD)	Event Time (hh:mm:ss.s)	Longitude ($^\circ$ E)	Latitude ($^\circ$ N)	Depth (km)	M_w	Tectonic Setting
1	2003-05-26	09:24:38.8	141.57	38.94	61.0	7.0	Intraslab
2	2011-04-07	14:32:50.6	141.85	38.32	53.3	7.1	
3	2005-08-16	02:46:40.3	142.05	38.24	37.0	7.2	Interplate
4	2008-07-19	02:39:34.8	142.42	37.47	21.8	6.9	
5	2012-12-07	08:18:34.9 08:18:46.9	144.09 143.83	38.01 37.77	57.8 19.5	7.2 7.2	Intraplate

Table: Earthquake details (from GCMT).



4. Methodology

Waveform inversion of teleseismic data

1. Kikuchi-Kanamori body-wave inversion program (Kikuchi and Kanamori, 1991) used for the analysis.
2. Moment Rate Function (MRF) generated from waveform modeling to validate the ERF algorithm.

Selection of strong-motion stations

1. Slip distribution, along with the seismic intensity distribution maps (JMA, 1996; ShakeMap, 2017), used to select stations within the inferred azimuthal range and seismic intensity > 3 .

6. Summary

1. HHT-based ERF captures the earthquake source energy release, with a **higher resolution** offered by HHT as compared to Fourier analysis methods and wavelet transform.
2. ERF retains frequency information, is computationally faster for a rapid interpretation of an event, and **does not entail assumptions** of the fault geometry and velocity structure. These are clear advantages over the traditional MRF.
3. ERF captures complex ruptures (2005 Miyagi-Oki event) and sub-events or

3. Data

Event Number	Event Date (YYYY-MM-DD)	Event Time (hh:mm:ss.s)	Longitude (°E)	Latitude (°N)	Depth (km)	M _w	Tectonic Setting
1	2003-05-26	09:24:38.8	141.57	38.94	61.0	7.0	Intraslab
2	2011-04-07	14:32:50.6	141.85	38.32	53.3	7.1	
3	2005-08-16	02:46:40.3	142.05	38.24	37.0	7.2	Interplate
4	2008-07-19	02:39:34.8	142.42	37.47	21.8	6.9	
5	2012-12-07	08:18:34.9	144.09	38.01	57.8	7.2	Intraplate
		08:18:46.9	143.83	37.77	19.5	7.2	

Table: Earthquake details (from GCMT).

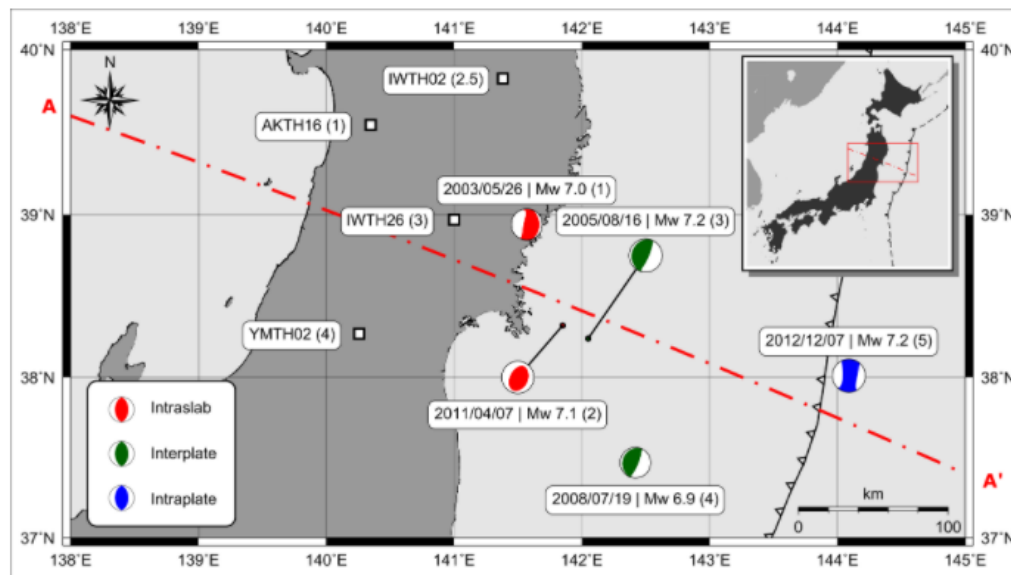
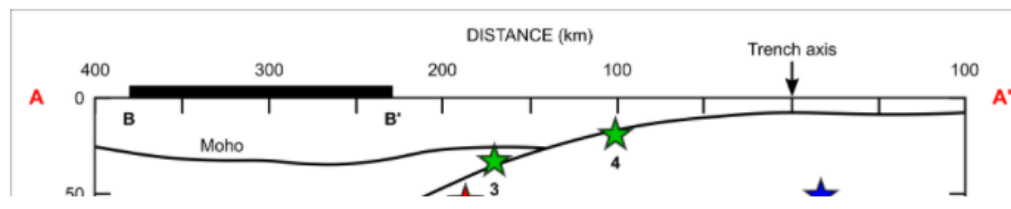


Figure: Map of the study region showing the five earthquakes and corresponding stations used for analysis.



4. Methodology

Waveform inversion of teleseismic data

1. Kikuchi-Kanamori body-wave inversion program (Kikuchi and Kanamori, 1991) used for the analysis.
2. Moment Rate Function (MRF) generated from waveform modeling to validate the ERF algorithm.

Selection of strong-motion stations

1. Slip distribution, along with the seismic intensity distribution maps (JMA, 1996; ShakeMap, 2017), used to select stations within the inferred azimuthal range and seismic intensity > 3.

6. Summary

1. HHT-based ERF captures the earthquake source energy release, with a higher resolution offered by HHT as compared to Fourier analysis methods and wavelet transform.
2. ERF retains frequency information, is computationally faster for a rapid interpretation of an event, and does not entail assumptions of the fault geometry and velocity structure. These are clear advantages over the traditional MRF.
3. ERF captures complex ruptures (2005 Miyagi-Oki event) and sub-events or

3. Data

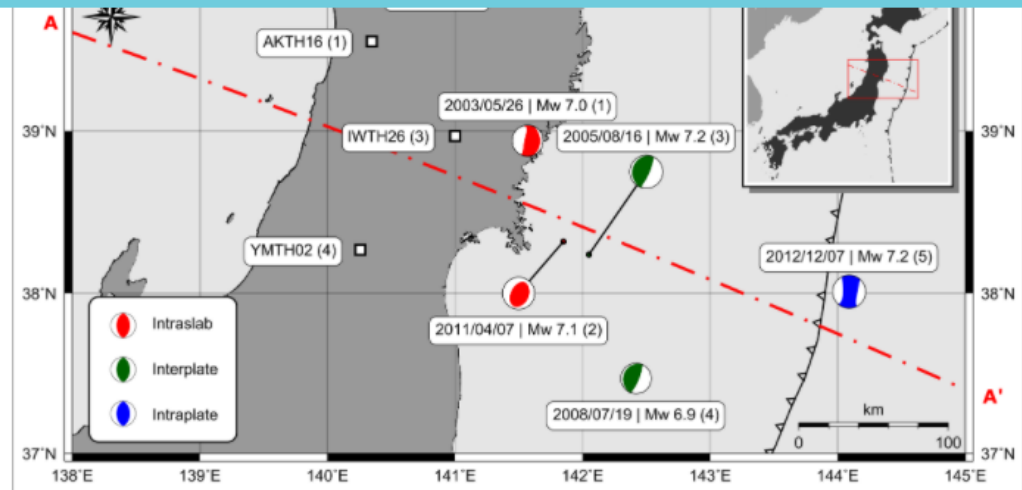


Figure: Map of the study region showing the five earthquakes and corresponding stations used for analysis.

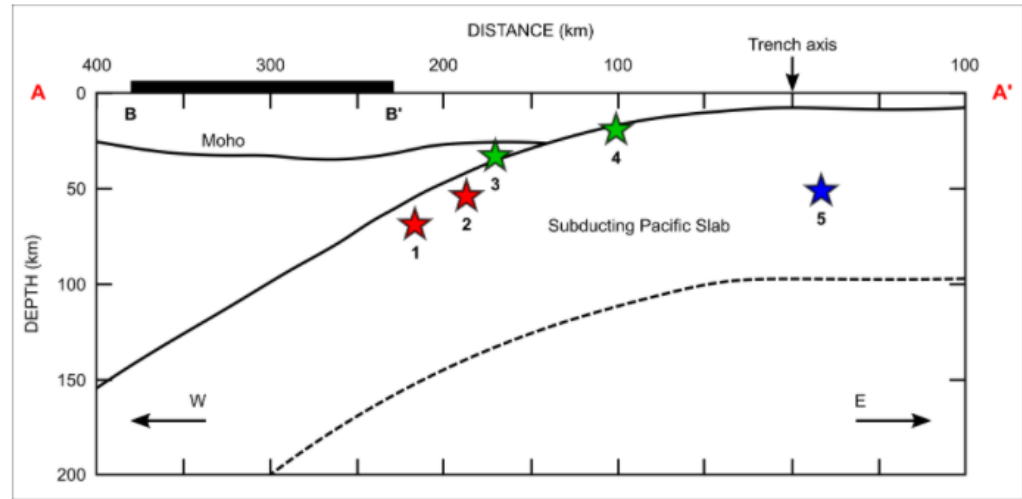


Figure: Cross-section showing the event distance from the trench, and depth, in km.

4. Methodology

Waveform inversion of teleseismic data

1. Kikuchi-Kanamori body-wave inversion program (Kikuchi and Kanamori, 1991) used for the analysis.
2. Moment Rate Function (MRF) generated from waveform modeling to validate the ERF algorithm.

Selection of strong-motion stations

1. Slip distribution, along with the seismic intensity distribution maps (JMA, 1996; ShakeMap, 2017), used to select stations within the inferred azimuthal range and seismic intensity > 3.

6. Summary

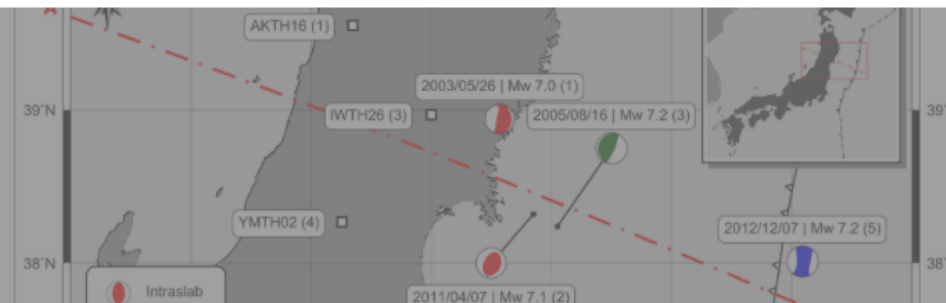
1. HHT-based ERF captures the earthquake source energy release, with a higher resolution offered by HHT as compared to Fourier analysis methods and wavelet transform.
2. ERF retains frequency information, is computationally faster for a rapid interpretation of an event, and does not entail assumptions of the fault geometry and velocity structure. These are clear advantages over the traditional MRF.
3. ERF captures complex ruptures (2005 Miyagi-Oki event) and sub-events or

3. Data

1. **Teleseismic data** from International Research Institutions for Seismology (IRIS). P and SH waveforms from 30-40 stations, epicentral distance 30° to 90°.

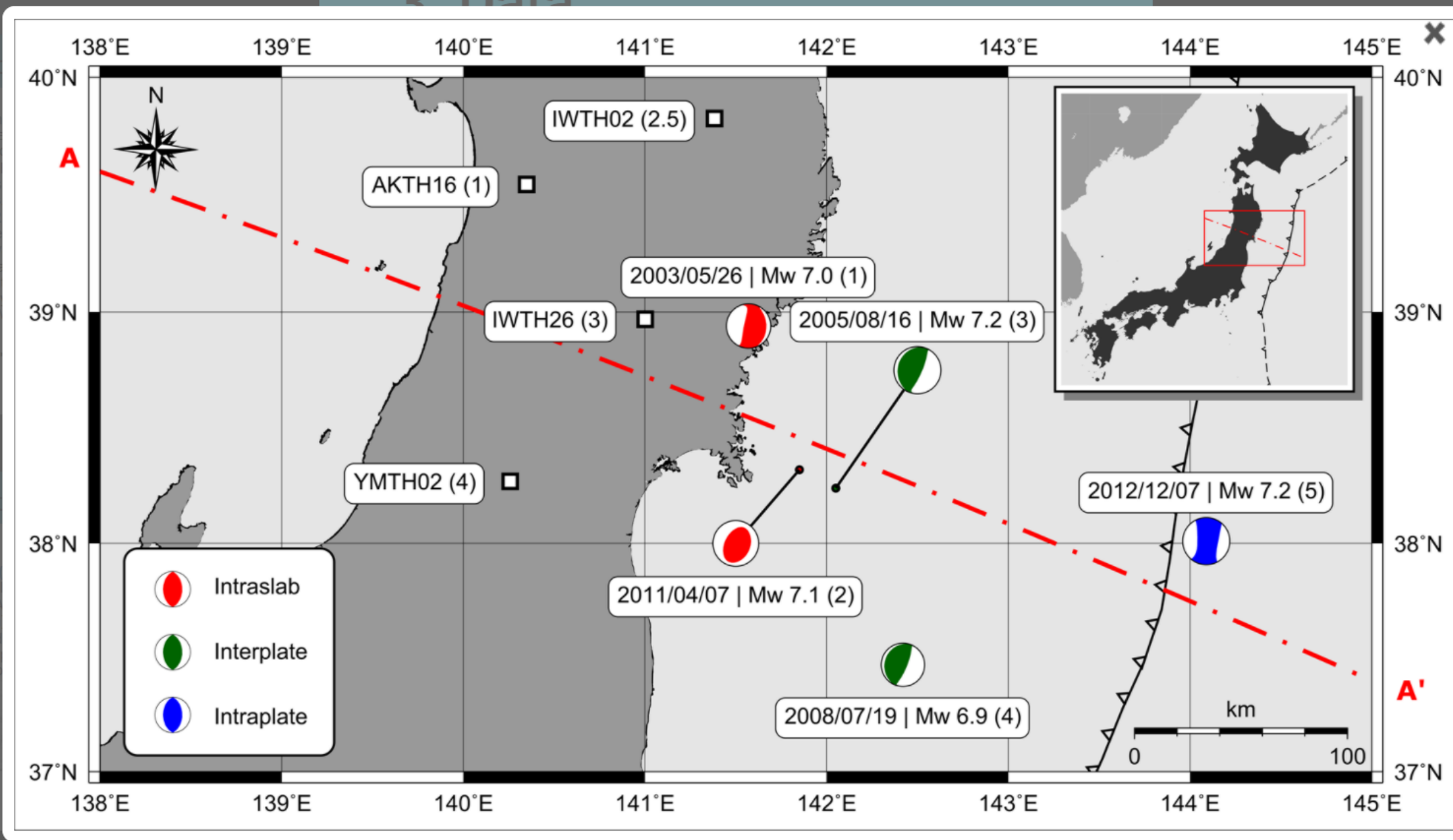
Event Number	Event Date (YYYY-MM-DD)	Event Time (hh:mm:ss.s)	Longitude (°E)	Latitude (°N)	Depth (km)	M _w	Tectonic Setting
1	2003-05-26	09:24:38.8	141.57	38.94	61.0	7.0	Intraslab
2	2011-04-07	14:32:50.6	141.85	38.32	53.3	7.1	
3	2005-08-16	02:46:40.3	142.05	38.24	37.0	7.2	Interplate
4	2008-07-19	02:39:34.8	142.42	37.47	21.8	6.9	
5	2012-12-07	08:18:34.9 08:18:46.9	144.09 143.83	38.01 37.77	57.8 19.5	7.2 7.2	Intraplate

1. 26 May 2003 Miyagi Intraslab Earthquake (Mw 7.0, depth 67.0 km)
 - Up-dip slip (towards east-northeast).
 - Station AKTH16, WNW (305.98° azimuth), seismic intensity (SI) 4.
 - Single, dominant, ~10 s energy pulse captured by both the ERF and MRF, along with a weaker tail.



1. HHT-based ERF captures the earthquake source energy release with a higher resolution offered by HHT as compared to Fourier analysis methods and wavelet transform.
2. ERF retains frequency information, is computationally faster for a rapid interpretation of an event, and does not entail assumptions of the fault geometry and velocity structure. These are clear advantages over the traditional MRF.
3. ERF captures complex ruptures (2005 Miyagi-Oki event) and sub-events or

3. Data



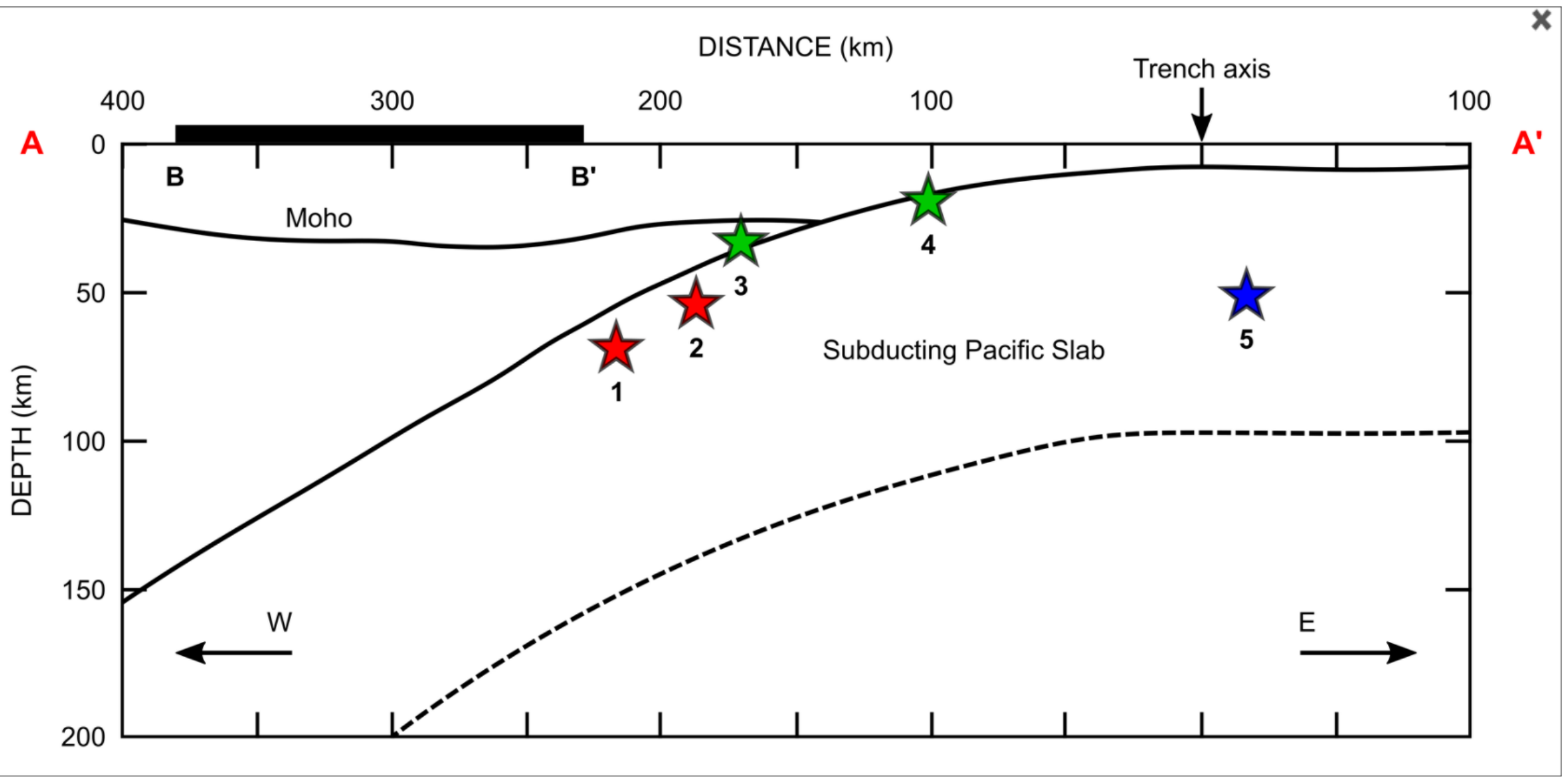
Subducting Pacific Slab

REFERENCES

CONTACT AUTHOR

GET IP

3 Data



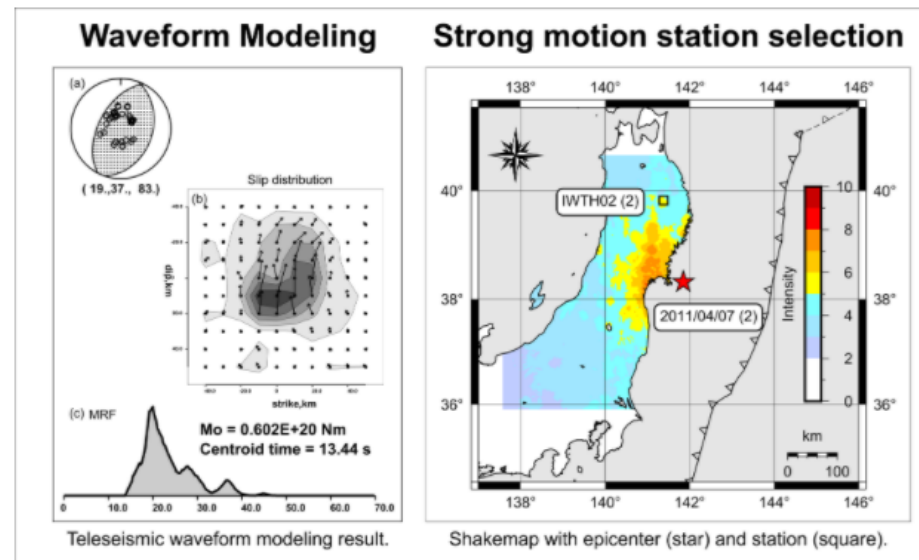
4. Methodology

Waveform inversion of teleseismic data

1. Kikuchi-Kanamori body-wave inversion program (Kikuchi and Kanamori, 1991) used for the analysis.
2. Moment Rate Function (MRF) generated from waveform modeling to validate the ERF algorithm.

Selection of strong-motion stations

1. Slip distribution, along with the seismic intensity distribution maps (JMA, 1996; ShakeMap, 2017), used to select stations within the inferred azimuthal range and seismic intensity > 3.



Key Points

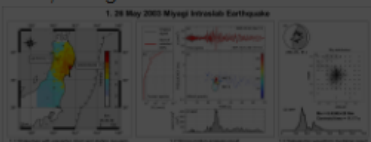
Specific Intrinsic Mode Functions (IMFs) represent energy release at the earthquake source. Energy Rate Functions (ERFs) generated from Hilbert spectral analysis of such IMF combinations. Proposed ERFs match well with the Moment Rate Functions (MRFs) from teleseismic waveform modeling. ERF-MRF match is controlled by the station azimuth and shaking intensity, and frequency and energy-based selection of IMFs.

OPEN

Results

16 May 2003 Miyagi Intralab Earthquake (Mw 7.0, depth 67.0 km)

- Up-dip slip (towards east-northeast).
- Station AKTH16, WNW (305.98° azimuth), seismic intensity (SI) 4.
- Single, dominant, ~10 s energy pulse captured by both the ERF and MRF, along with a weaker tail.



OPEN

4. Methodology

Waveform inversion of teleseismic data

1. Kikuchi-Kanamori body-wave inversion program (Kikuchi and Kanamori, 1991) used for the analysis.
2. Moment Rate Function (MRF) generated from waveform modeling to validate the ERF algorithm.

Selection of strong-motion stations

1. Slip distribution, along with the seismic intensity distribution maps (JMA, 1996; ShakeMap, 2017), used to select stations within the inferred azimuthal range and seismic intensity > 3.

OPEN

6. Summary

1. HHT-based ERF captures the earthquake source energy release, with a higher resolution offered by HHT as compared to Fourier analysis methods and wavelet transform.
2. ERF retains frequency information, is computationally faster for a rapid interpretation of an event, and does not entail assumptions of the fault geometry and velocity structure. These are clear advantages over the traditional MRF.
3. ERF captures complex ruptures (2005 Miyagi-Oki event) and sub-events or

OPEN

4. Methodology

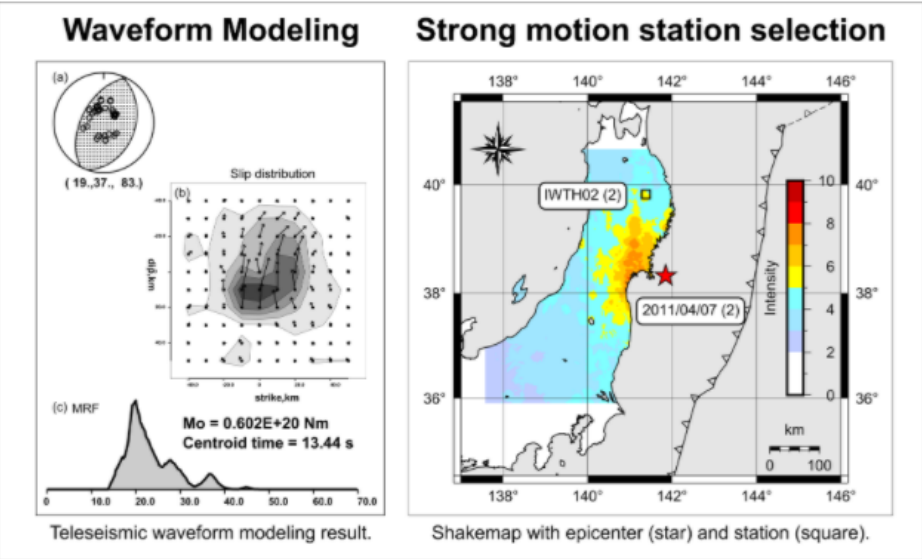


Figure: Waveform modeling results. Shakemap (along with slip distribution), used for strong-motion station-selection.

HHT-based strong-motion analysis

1. Hilbert-Huang Transform (HHT) is a combination of Empirical Mode Decomposition (EMD) and Hilbert Spectral Analysis (HSA) (Huang et al., 1998).
2. EMD decomposes the data into multiple frequency components (IMFs).
3. IMFs selected in the frequency range 0.1 to 3 Hz. Hilbert energy spectrum, a time-frequency-energy

4. Methodology

Waveform inversion of teleseismic data

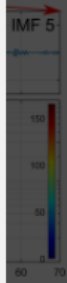
1. Kikuchi-Kanamori body-wave inversion program (Kikuchi and Kanamori, 1991) used for the analysis.
2. Moment Rate Function (MRF) generated from waveform modeling to validate the ERF algorithm.

Selection of strong-motion stations

1. Slip distribution, along with the seismic intensity distribution maps (JMA, 1996; ShakeMap, 2017), used to select stations within the inferred azimuthal range and seismic intensity > 3.

6. Summary

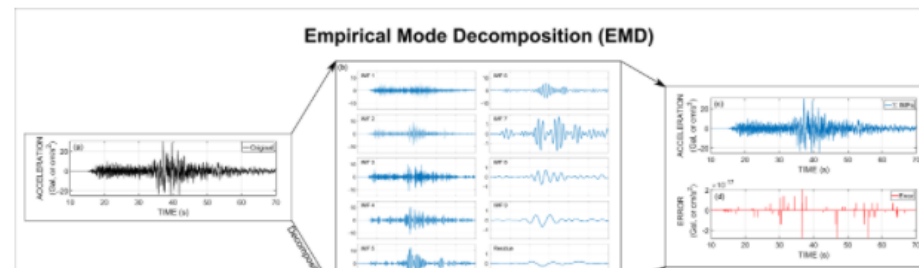
1. HHT-based ERF captures the earthquake source energy release, with a higher resolution offered by HHT as compared to Fourier analysis methods and wavelet transform.
2. ERF retains frequency information, is computationally faster for a rapid interpretation of an event, and does not entail assumptions of the fault geometry and velocity structure. These are clear advantages over the traditional MRF.
3. ERF captures complex ruptures (2005 Miyagi-Oki event) and sub-events or



4. Methodology

HHT-based strong-motion analysis

1. Hilbert-Huang Transform (HHT) is a combination of Empirical Mode Decomposition (**EMD**) and Hilbert Spectral Analysis (**HSA**) (Huang et al., 1998).
2. EMD decomposes the data into multiple frequency components (IMFs).
3. **IMFs** selected in the **frequency range 0.1 to 3 Hz**. Hilbert energy spectrum, a time-frequency-energy representation of the signal, generated for each selected IMF.
4. **Maximum amplitude-squared values** obtained from the Hilbert spectra of selected IMFs used to generate the Energy Rate Function (ERF).
5. ERF is representative of energy release at the earthquake source, validated by its comparison with the MRF.



4. Methodology

Waveform inversion of teleseismic data

1. Kikuchi-Kanamori body-wave inversion program (Kikuchi and Kanamori, 1991) used for the analysis.
2. Moment Rate Function (MRF) generated from waveform modeling to validate the ERF algorithm.

Selection of strong-motion stations

1. Slip distribution, along with the seismic intensity distribution maps (JMA, 1996; ShakeMap, 2017), used to select stations within the inferred azimuthal range and seismic intensity > 3.

6. Summary

1. HHT-based **ERF captures the earthquake source energy release**, with a **higher resolution** offered by HHT as compared to Fourier analysis methods and wavelet transform.
2. **ERF retains frequency information**, is computationally faster for a rapid interpretation of an event, and **does not entail assumptions** of the fault geometry and velocity structure. These are clear advantages over the traditional MRF.
3. **ERF captures complex ruptures** (2005 Miyagi-Oki event) and sub-events or

4. Methodology

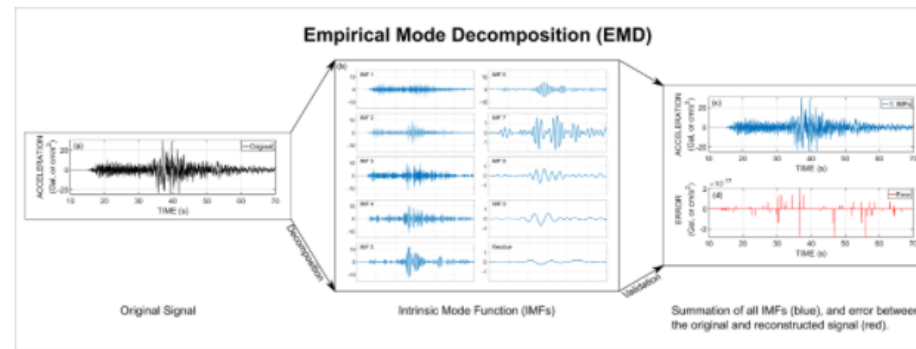


Figure: EMD and validation.

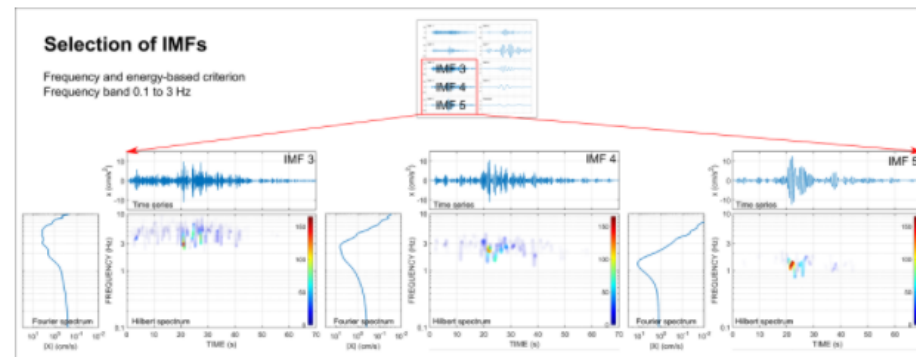
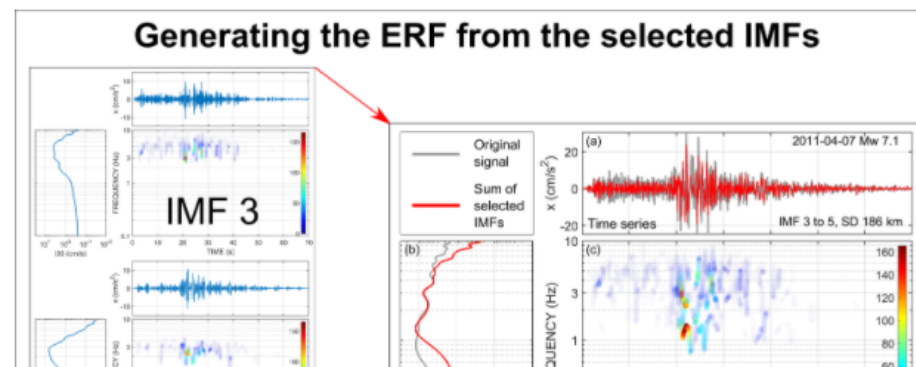


Figure: Selection of IMFs.



Key Points

Specific Intrinsic Mode Functions (IMFs) represent energy release at the earthquake source.

Energy Rate Functions (ERFs) generated from Hilbert spectral analysis of such IMF combinations.

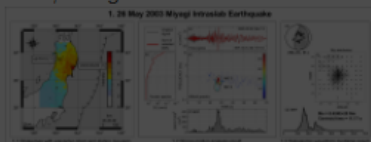
Proposed ERFs match well with the Moment Rate Functions (MRFs) from teleseismic waveform modeling.

ERF-MRF match is controlled by the station azimuth and shaking intensity, and frequency and energy-based selection of IMFs.

Results

26 May 2003 Miyagi Intralab Earthquake (Mw 7.0, depth 67.0 km)

- Up-dip slip (towards east-northeast).
- Station AKTH16, WNW (305.98° azimuth), seismic intensity (SI) 4.
- Single, dominant, ~10 s energy pulse captured by both the ERF and MRF, along with a weaker tail.



4. Methodology

Waveform inversion of teleseismic data

1. Kikuchi-Kanamori body-wave inversion program (Kikuchi and Kanamori, 1991) used for the analysis.
2. Moment Rate Function (MRF) generated from waveform modeling to validate the ERF algorithm.

Selection of strong-motion stations

1. Slip distribution, along with the seismic intensity distribution maps (JMA, 1996; ShakeMap, 2017), used to select stations within the inferred azimuthal range and seismic intensity > 3.

6. Summary

1. HHT-based ERF captures the earthquake source energy release, with a **higher resolution** offered by HHT as compared to Fourier analysis methods and wavelet transform.
2. ERF retains frequency information, is computationally faster for a rapid interpretation of an event, and **does not entail assumptions** of the fault geometry and velocity structure. These are clear advantages over the traditional MRF.
3. ERF captures complex ruptures (2005 Miyagi-Oki event) and sub-events or

4. Methodology

Generating the ERF from the selected IMFs

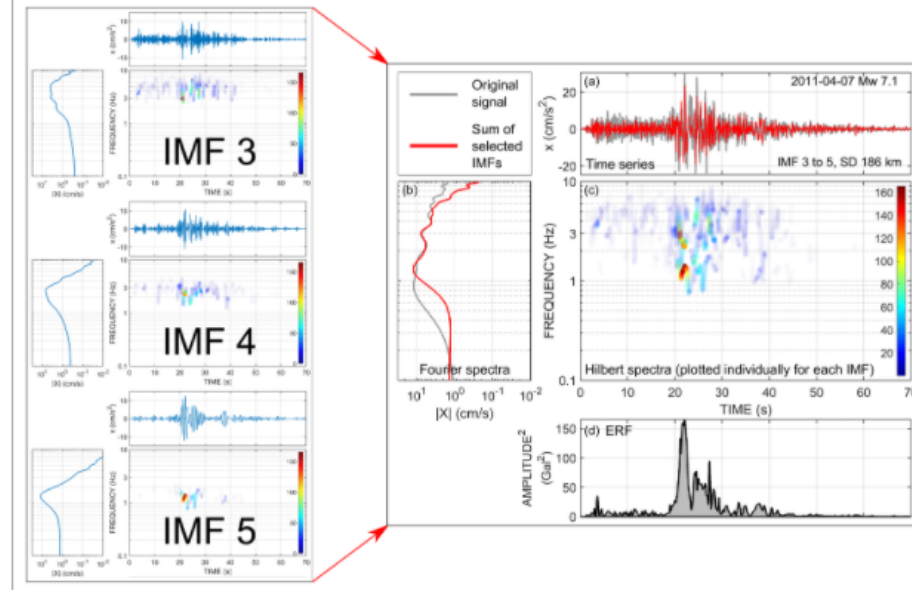
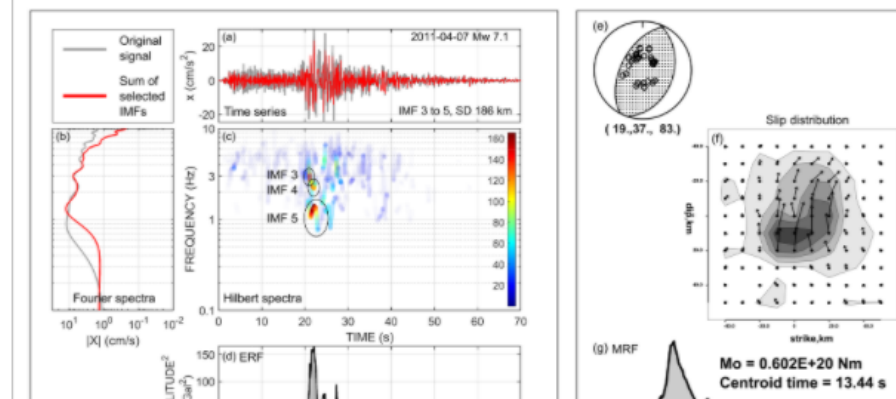


Figure: Using the selected IMFs to generate the Energy Rate Function (ERF).

Comparing the ERF and MRF



4. Methodology

Waveform inversion of teleseismic data

1. Kikuchi-Kanamori body-wave inversion program (Kikuchi and Kanamori, 1991) used for the analysis.
2. Moment Rate Function (MRF) generated from waveform modeling to validate the ERF algorithm.

Selection of strong-motion stations

1. Slip distribution, along with the seismic intensity distribution maps (JMA, 1996; ShakeMap, 2017), used to select stations within the inferred azimuthal range and seismic intensity > 3 .

6. Summary

1. HHT-based ERF captures the earthquake source energy release, with a higher resolution offered by HHT as compared to Fourier analysis methods and wavelet transform.
2. ERF retains frequency information, is computationally faster for a rapid interpretation of an event, and does not entail assumptions of the fault geometry and velocity structure. These are clear advantages over the traditional MRF.
3. ERF captures complex ruptures (2005 Miyagi-Oki event) and sub-events or

Figure 1 displays the analysis of the time series of the magnetic field component X . The figure is divided into two main panels. The left panel shows the decomposition of the time series into five Intrinsic Mode Functions (IMFs), labeled IMF 3, IMF 4, and IMF 5. Each IMF plot includes a time series (X in cm/s) and a corresponding Hilbert spectrum (Amplitude² in Gauss²) plotted against time (s) and frequency (Hz). The right panel shows the original time series (X in cm/s) and its Hilbert spectrum. A red arrow points from the Hilbert spectrum of IMF 4 to the Hilbert spectrum of the original time series, indicating the contribution of IMF 4 to the overall signal.

Comparing the ERF and MRF

The figure is divided into four quadrants, each showing a different aspect of the seismic analysis:

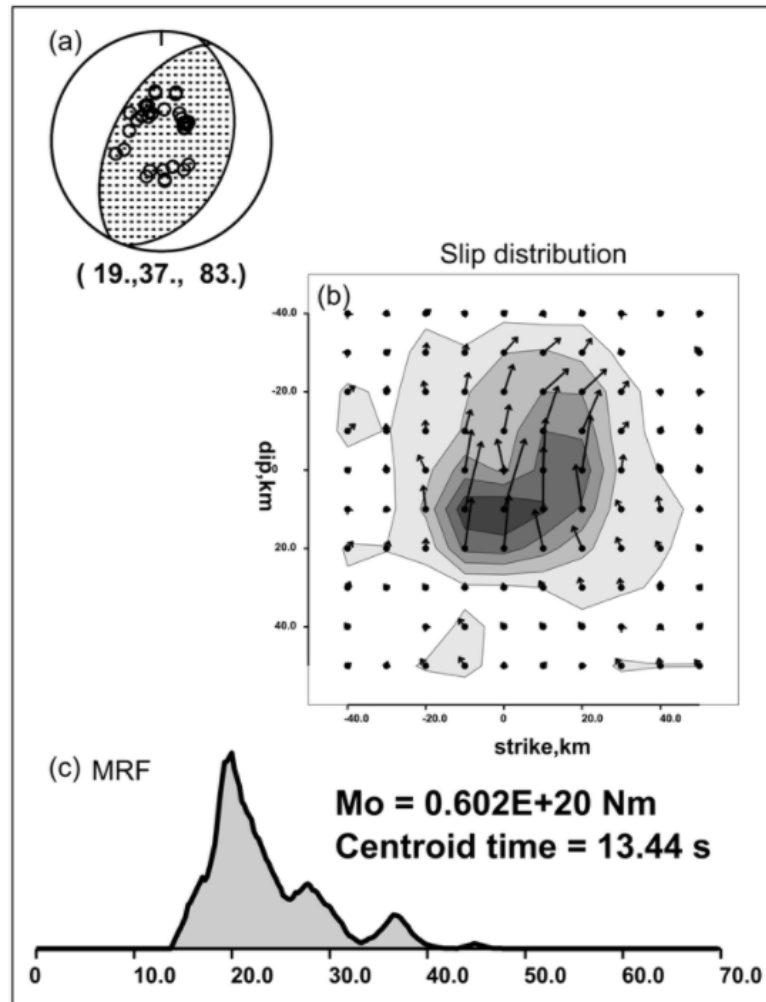
- Top-left:** Time series (a) and Hilbert spectra (c). The time series shows the original signal (grey) and the sum of selected IMFs (red). The Hilbert spectra show the frequency content (0.1 to 3 Hz) over time (0 to 70 s) for IMF 3, 4, and 5. A color bar indicates amplitude from 20 to 160.
- Top-right:** Slip distribution (f). A map showing the slip distribution on a fault plane, with a color scale from 0 to 160 cm/s.
- Bottom-left:** Fourier spectra (b). A plot of the Fourier spectra of the original signal (grey) and the sum of selected IMFs (red) over a frequency range from 10^{-1} to 10^{-2} cm/s.
- Bottom-right:** MRF (g). A plot of the MRF waveform model, showing the amplitude (0 to 150) versus time (0 to 70 s). The model is labeled with $M_0 = 0.602E+20$ Nm and Centroid time = 13.44 s.

Strong motion analysis result.

Teleseismic waveform modeling result.

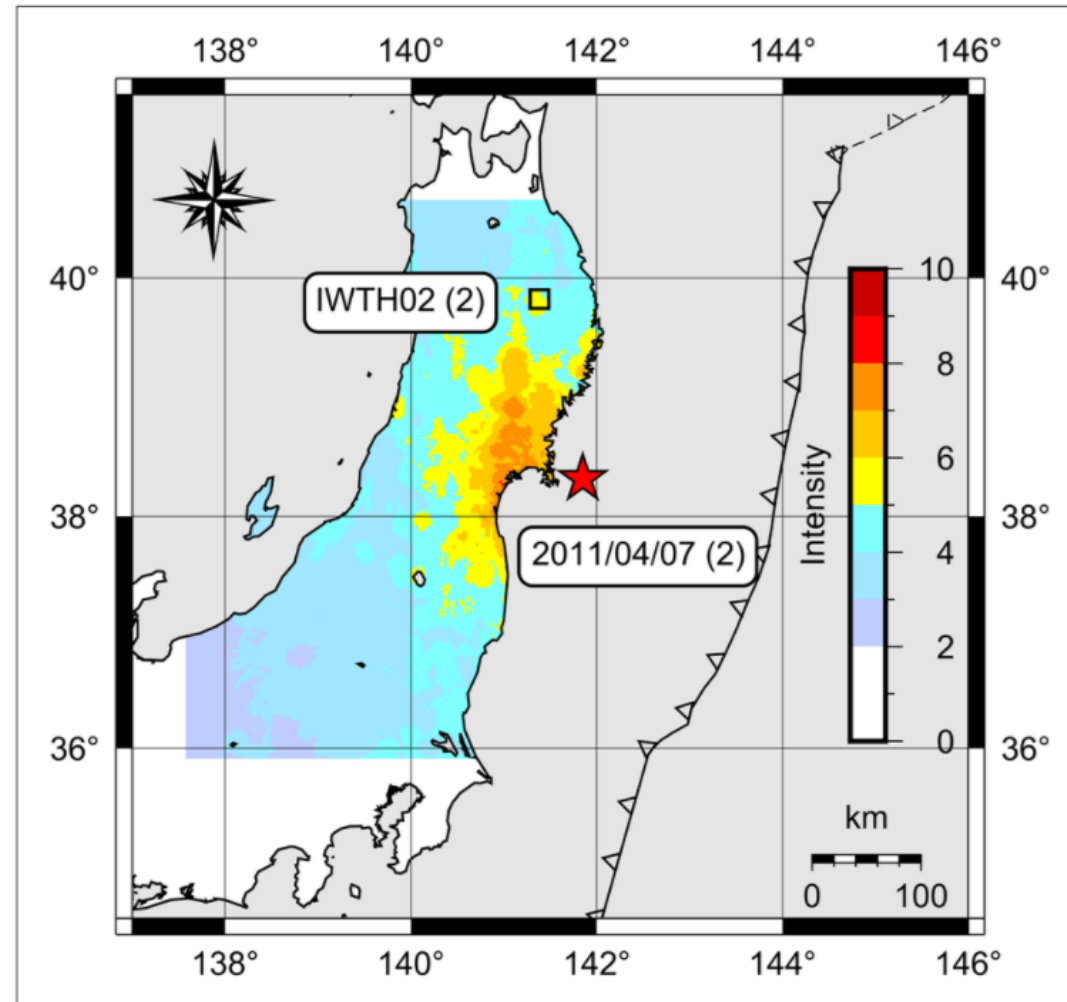
1. HHT-based **ERF captures the earthquake source energy release**, with a **higher resolution** offered by HHT as compared to Fourier analysis methods and wavelet transform.
2. **ERF retains frequency information**, is computationally faster for a rapid interpretation of an event, and **does not entail assumptions** of the fault geometry and velocity structure. These are clear advantages over the traditional MRF.
3. **ERF captures complex ruptures** (2005 Miyagi-Oki event) and sub-events or

Waveform Modeling



Teleseismic waveform modeling result.

Strong motion station selection



Shakemap with epicenter (star) and station (square).

4. Methodology

Hilbert spectra of selected IMFs used to generate the Energy Rate Function (ERF)

Empirical Mode Decomposition (EMD)

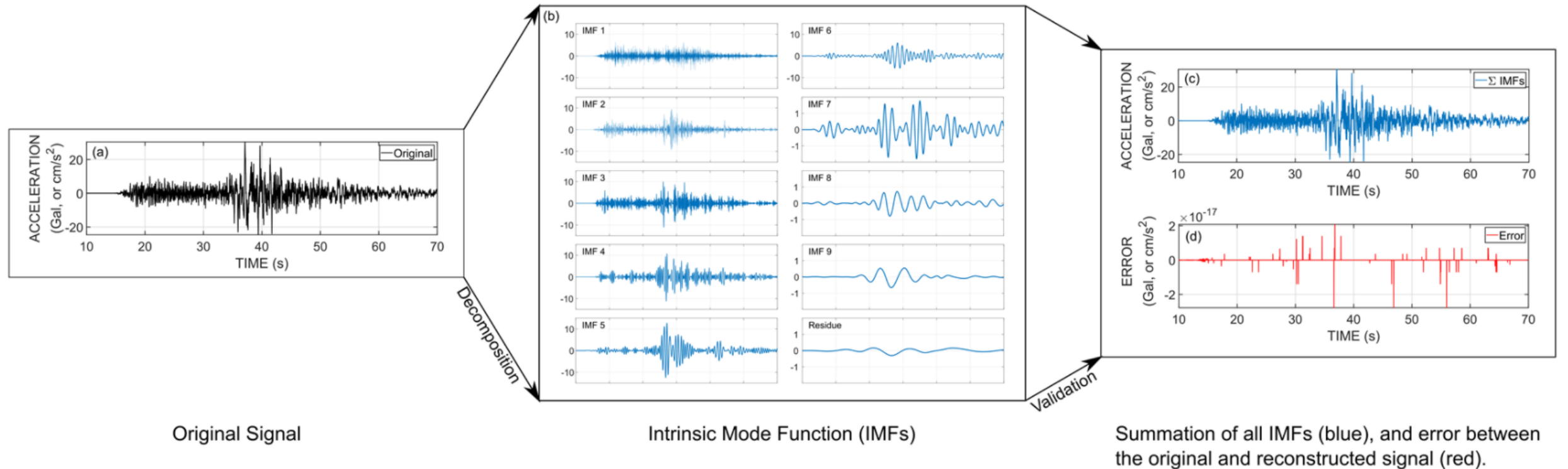


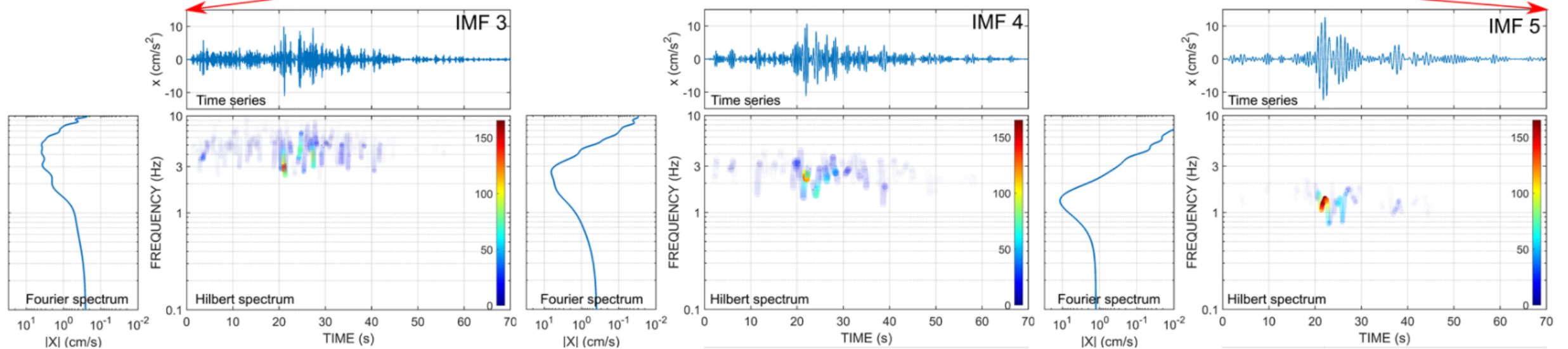
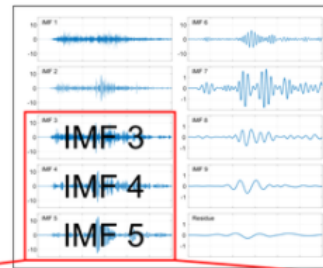
Figure: Selection of IMFs.

Generating the ERF from the selected IMFs

4. Methodology

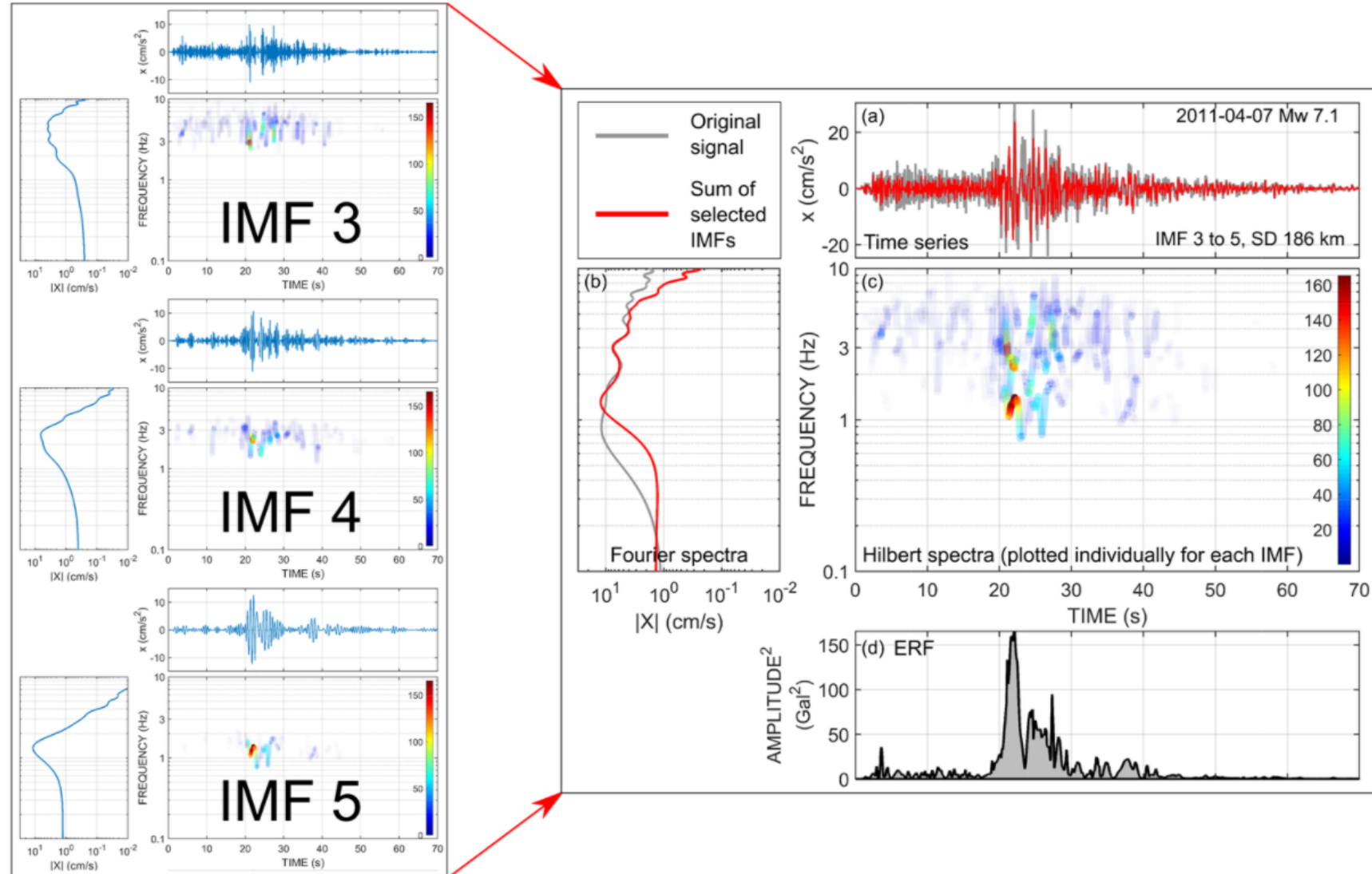
Selection of IMFs

Frequency and energy-based criterion
Frequency band 0.1 to 3 Hz



4 Methodology

Generating the ERF from the selected IMFs



1. Key Points

1. Specific Intrinsic Mode Functions (IMFs) represent energy release at the earthquake source.
2. Energy Rate Functions (ERFs) from Hilbert spectral analysis combinations.
3. Proposed ERFs match well with Moment Rate Functions (MRFs) in teleseismic waveform modeling.
4. ERF-MRF match is controlled by station azimuth and shaking intensity and frequency and energy-based selection of IMFs.

A short video explaining our work

OPEN

5. Results

1. 26 May 2003 Miyagi Intraslab Earthquake (Mw 7.0, depth 10 km)
 - Up-dip slip (towards east)
 - Station AKTH16, WNW (10° azimuth), seismic intensity 10
 - Single, dominant, ~10 s pulse captured by both the MRF, along with a weaker

1. 26 May 2003 Miyagi Intraslab Earthquake

OPEN

Methodology

The ERF (MRF) generated from the teleseismic waveform modeling to validate the ERF. The ERF, along with the seismic distribution maps (JMA, 1996; 2017), used to select stations preferred azimuthal range and intensity > 3.

Strong motion station selection

OPEN

Summary

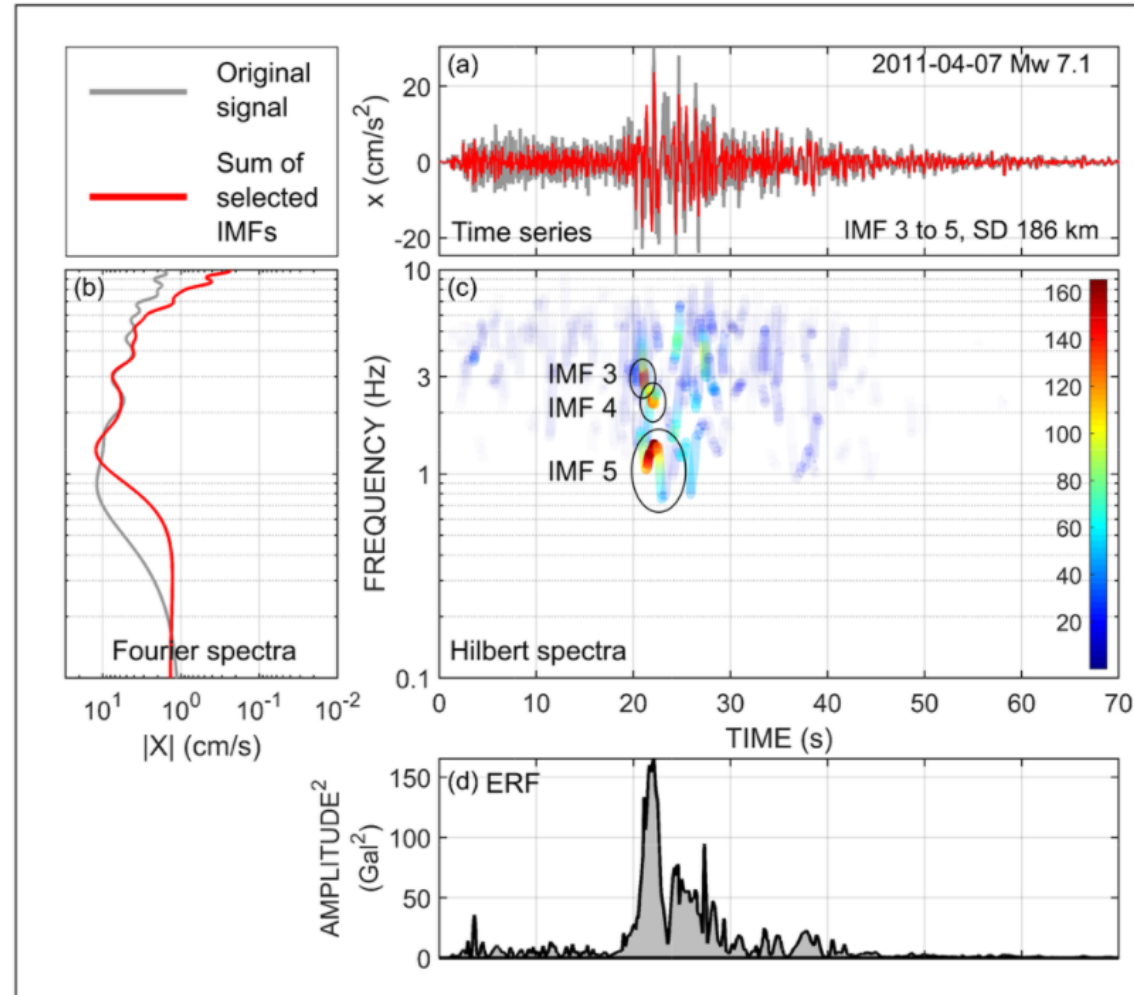
ERF captures the source energy release, offering higher resolution than Fourier analysis methods. ERF captures the frequency information, is faster for a rapid event, and does not require assumptions of the fault geometry and velocity structure. These are advantages over the traditional MRF.

ERF captures complex ruptures (2005 event) and sub-events or

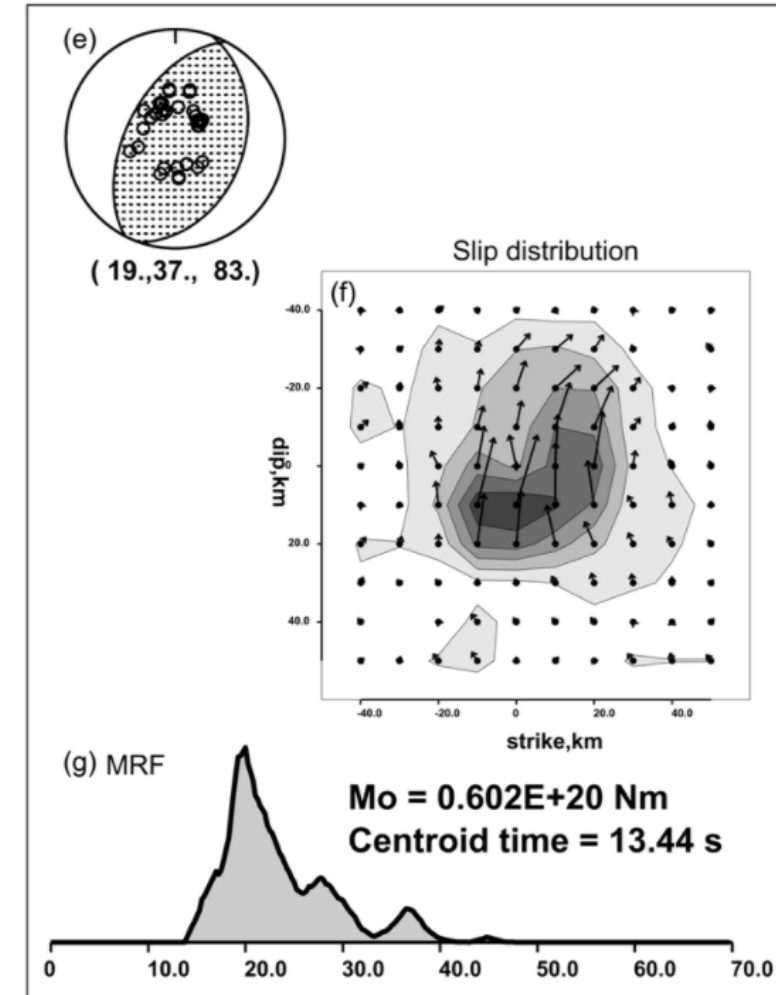
OPEN

4. Methodology

Comparing the ERF and MRF



Strong motion analysis result.



Teleseismic waveform modeling result.

1. Key P

1. Specific Intr...
2. Energy Rate...
3. Proposed ERF...
4. ERF-MRF...

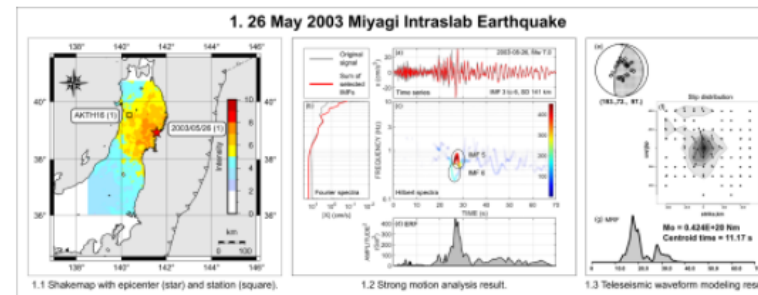
5. Result

1. 26 May 2003 Earthquake
- Up-dip s...
- Station / azimuth...
- Single, pulse ca...

5. Results

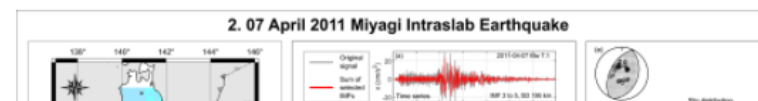
1. 26 May 2003 Miyagi Intralab Earthquake (Mw 7.0, depth 67.0 km)

- Up-dip slip (towards east-northeast).
- Station AKTH16, WNW (305.98° azimuth), seismic intensity (SI) 4.
- Single, dominant, ~10 s energy pulse captured by both the ERF and MRF, along with a weaker tail.



2. 07 April 2011 Miyagi Intralab Earthquake (Mw 7.1, depth 53.3 km)

- Slip direction northwest.
- Station IWTH02, north-northwest (345.73° azimuth), SI 6-lower.
- Single, dominant energy pulse with a peak at 20 seconds and decaying gradually up to 40 seconds captured by both the ERF and MRF.



1. Key Points

1. Specific Intrinsic Mode Functions (IMFs) represent energy release at the earthquake source.
2. Energy Rate Functions (ERFs) generated from Hilbert spectral analysis of such IMF combinations.
3. Proposed ERFs match well with the Moment Rate Functions (MRFs) from teleseismic waveform modeling.
4. ERF-MRF match is controlled by the station azimuth and shaking intensity, and frequency and energy-based selection of IMFs.

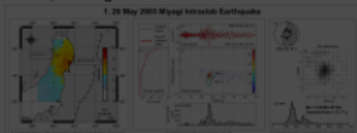
A short video explaining our work

OPEN

5. Results

1. 26 May 2003 Miyagi Intralab Earthquake (Mw 7.0, depth 67.0 km)

- Up-dip slip (towards east-northeast).
- Station AKTH16, WNW (305.98° azimuth), seismic intensity (SI) 4.
- Single, dominant, ~10 s energy pulse captured by both the ERF and MRF, along with a weaker tail.



OPEN

4. Methodology

2. Moment Rate Function (MRF) generated from waveform modeling to validate the ERF algorithm.

Selection of strong-motion stations

1. Slip distribution, along with the seismic intensity distribution maps (JMA, 1996; ShakeMap, 2017), used to select stations within the inferred azimuthal range and seismic intensity > 3.



OPEN

6. Summary

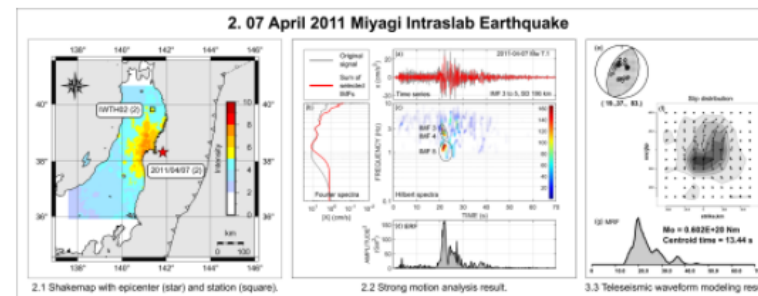
1. HHT-based ERF captures the earthquake source energy release, with a **higher resolution** offered by HHT as compared to Fourier analysis methods and wavelet transform.
2. ERF retains frequency information, is computationally faster for a rapid interpretation of an event, and **does not entail assumptions** of the fault geometry and velocity structure. These are clear advantages over the traditional MRF.
3. ERF captures complex ruptures (2005 Miyagi-Oki event) and sub-events or

OPEN

5. Results

2. 07 April 2011 Miyagi Intralab Earthquake (Mw 7.1, depth 53.3 km)

- Slip direction northwest.
- Station IWTH02, north-northwest (345.73° azimuth), SI 6-lower.
- Single, dominant energy pulse with a peak at 20 seconds and decaying gradually up to 40 seconds captured by both the ERF and MRF.



3. 16 August 2005 Miyagi-Oki Interplate Earthquake (Mw 7.2, depth 37.0 km)

- Station IWTH26, azimuth 309.76° , SI 5-upper.
- **Rough MRF** observed by [Lay et al. \(2012\)](#) and [Yaginuma et al. \(2006\)](#).
- ERF and MRF both match well with the above studies.
- A deeper interplate event, and shows **enrichment in high-frequency energy** (0.4 to 5 Hz range).

Figure 3: 16 August 2005 Miyagi-Oki Interplate Earthquake

4. Methodology

2. Moment Rate Function (MRF) generated from waveform modeling to validate the ERF algorithm.

Selection of strong-motion stations

1. Slip distribution, along with the seismic intensity distribution maps ([JMA, 1996](#); [ShakeMap, 2017](#)), used to select stations within the inferred azimuthal range and seismic intensity > 3 .



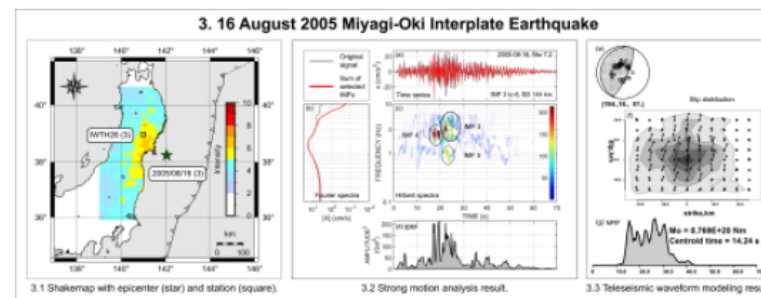
6. Summary

1. HHT-based ERF captures the earthquake source energy release, with a **higher resolution** offered by HHT as compared to Fourier analysis methods and wavelet transform.
2. ERF retains frequency information, is computationally faster for a rapid interpretation of an event, and **does not entail assumptions** of the fault geometry and velocity structure. These are clear advantages over the traditional MRF.
3. ERF captures complex ruptures (2005 Miyagi-Oki event) and sub-events or

5. Results

3. 16 August 2005 Miyagi-Oki Interplate Earthquake (Mw 7.2, depth 37.0 km)

- Station IWTH26, azimuth 309.76°, SI 5-upper.
- **Rough MRF** observed by [Lay et al. \(2012\)](#) and [Yaginuma et al. \(2006\)](#).
- ERF and MRF both match well with the above studies.
- A deeper interplate event, and shows **enrichment in high-frequency energy** (0.4 to 5 Hz range).



4. 19 July 2008 Fukushima ken-Oki Interplate Earthquake (Mw 6.9, depth 21.8 km)

- Slip directed up-dip (east-southeast).
- Station YMTH02, north-northwest (azimuth 295.96°), SI 3.
- **ERF-MRF match** obtained even for **low SI** at the station location.
- A shallow interplate event; **low-frequency energy**

1. Key Points

1. Specific Intrinsic Mode Functions (IMFs) represent energy release at the earthquake source.
2. Energy Rate Functions (ERFs) generated from Hilbert spectral analysis of such IMF combinations.
3. Proposed ERFs match well with the Moment Rate Functions (MRFs) from teleseismic waveform modeling.
4. ERF-MRF match is controlled by the station azimuth and shaking intensity, and frequency and energy-based selection of IMFs.

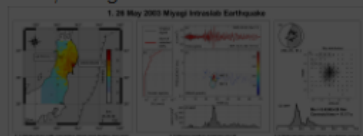
A short video explaining our work:

OPEN

5. Results

1. 26 May 2003 Miyagi Intraslab Earthquake (Mw 7.0, depth 67.0 km)

- Up-dip slip (towards east-northeast).
- Station AKTH16, WNW (305.98° azimuth), seismic intensity (SI) 4.
- Single, dominant, ~10 s energy pulse captured by both the ERF and MRF, along with a weaker tail.



OPEN

4. Methodology

2. Moment Rate Function (MRF) generated from waveform modeling to validate the ERF algorithm.

Selection of strong-motion stations

1. Slip distribution, along with the seismic intensity distribution maps ([JMA, 1996](#); [ShakeMap, 2017](#)), used to select stations within the inferred azimuthal range and seismic intensity > 3.



OPEN

6. Summary

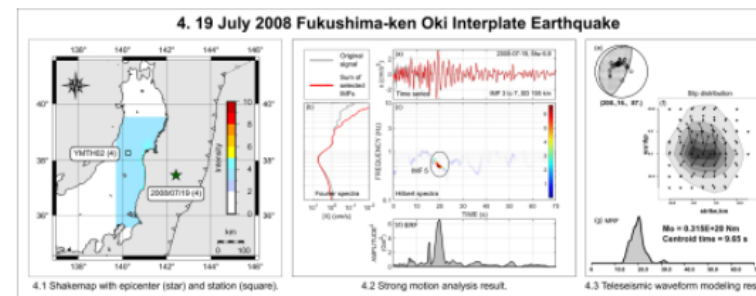
1. HHT-based ERF captures the **earthquake source energy release**, with a **higher resolution** offered by HHT as compared to Fourier analysis methods and wavelet transform.
2. **ERF retains frequency information**, is computationally faster for a rapid interpretation of an event, and **does not entail assumptions** of the fault geometry and velocity structure. These are clear advantages over the traditional MRF.
3. **ERF captures complex ruptures** (2005 Miyagi-Oki event) and sub-events or

OPEN

5. Results

4. 19 July 2008 Fukushima ken-Oki Interplate Earthquake (Mw 6.9, depth 21.8 km)

- Slip directed up-dip (east-southeast).
- Station YMTH02, north-northwest (azimuth 295.96°), SI 3.
- **ERF-MRF match** obtained even for **low SI** at the station location.
- A shallow interplate event; **low-frequency energy** (Ye et al., 2013).



5. 07 December 2012 Kamaishi Intraplate Earthquake (Mw 7.2, depth 50.8 km)

- Station IWTH02, azimuth 313.85°, SI 5-lower. Station approximately orthogonal to strike.
- Earthquake modeled as two independent events, deep thrust and shallow normal-faulting (Craig et al., 2014; Harada et al., 2013; Lay et al., 2013).
- **ERF and MRF** both show **two distinct pulses**,

1. Key Points

1. Specific Intrinsic Mode Functions (IMFs) represent energy release at the earthquake source.
2. Energy Rate Functions (ERFs) generated from Hilbert spectral analysis of such IMF combinations.
3. Proposed ERFs match well with the Moment Rate Functions (MRFs) from teleseismic waveform modeling.
4. ERF-MRF match is controlled by the station azimuth and shaking intensity, and frequency and energy-based selection of IMFs.

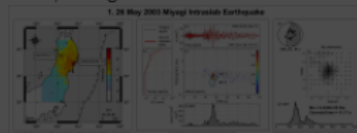
A short video explaining our work

OPEN

5. Results

1. 26 May 2003 Miyagi Intraslab Earthquake (Mw 7.0, depth 67.0 km)

- Up-dip slip (towards east-northeast).
- Station AKTH16, WNW (305.98° azimuth), seismic intensity (SI) 4.
- Single, dominant, ~10 s energy pulse captured by both the ERF and MRF, along with a weaker tail.



OPEN

4. Methodology

2. Moment Rate Function (MRF) generated from waveform modeling to validate the ERF algorithm.

Selection of strong-motion stations

1. Slip distribution, along with the seismic intensity distribution maps (JMA, 1996; ShakeMap, 2017), used to select stations within the inferred azimuthal range and seismic intensity > 3.



OPEN

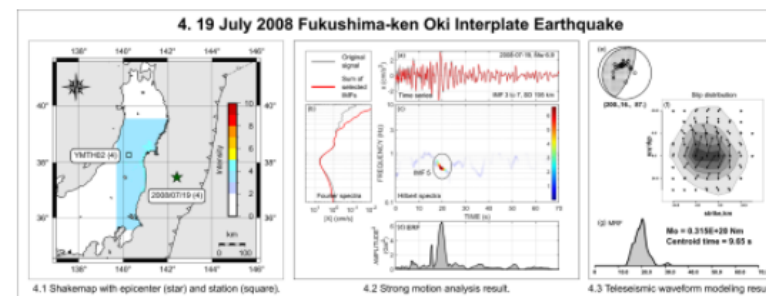
6. Summary

1. HHT-based ERF captures the earthquake source energy release, with a **higher resolution** offered by HHT as compared to Fourier analysis methods and wavelet transform.
2. ERF retains frequency information, is computationally faster for a rapid interpretation of an event, and **does not entail assumptions** of the fault geometry and velocity structure. These are clear advantages over the traditional MRF.
3. ERF captures complex ruptures (2005 Miyagi-Oki event) and sub-events or

OPEN

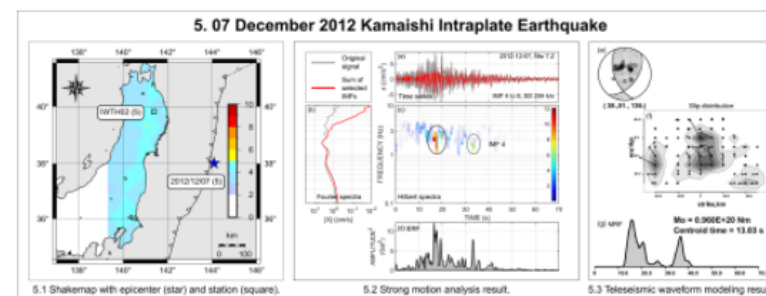
5. Results

(Ye et al., 2013).



5. 07 December 2012 Kamaishi Intraplate Earthquake (Mw 7.2, depth 50.8 km)

- Station IWTH02, azimuth 313.85°, SI 5-lower. Station approximately orthogonal to strike.
- Earthquake modeled as two independent events, deep thrust and shallow normal-faulting (Craig et al., 2014; Harada et al., 2013; Lay et al., 2013).
- ERF and MRF both show **two distinct pulses**, possibly representing the two events.



1. Key Points

1. Specific Intrinsic Mode Functions (IMFs) represent energy release at the earthquake source.
2. Energy Rate Functions (ERFs) generated from Hilbert spectral analysis of such IMF combinations.
3. Proposed ERFs match well with the Moment Rate Functions (MRFs) from teleseismic waveform modeling.
4. ERF-MRF match is controlled by the station azimuth and shaking intensity, and frequency and energy-based selection of IMFs.

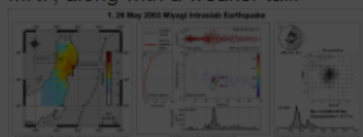
A short video explaining our work:

OPEN

5. Results

1. 26 May 2003 Miyagi Intraslab Earthquake (Mw 7.0, depth 67.0 km)

- Up-dip slip (towards east-northeast).
- Station AKTH16, WNW (305.98° azimuth), seismic intensity (SI) 4.
- Single, dominant, ~10 s energy pulse captured by both the ERF and MRF, along with a weaker tail.



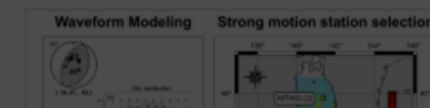
OPEN

4. Methodology

2. Moment Rate Function (MRF) generated from waveform modeling to validate the ERF algorithm.

Selection of strong-motion stations

1. Slip distribution, along with the seismic intensity distribution maps (JMA, 1996; ShakeMap, 2017), used to select stations within the inferred azimuthal range and seismic intensity > 3.



OPEN

6. Summary

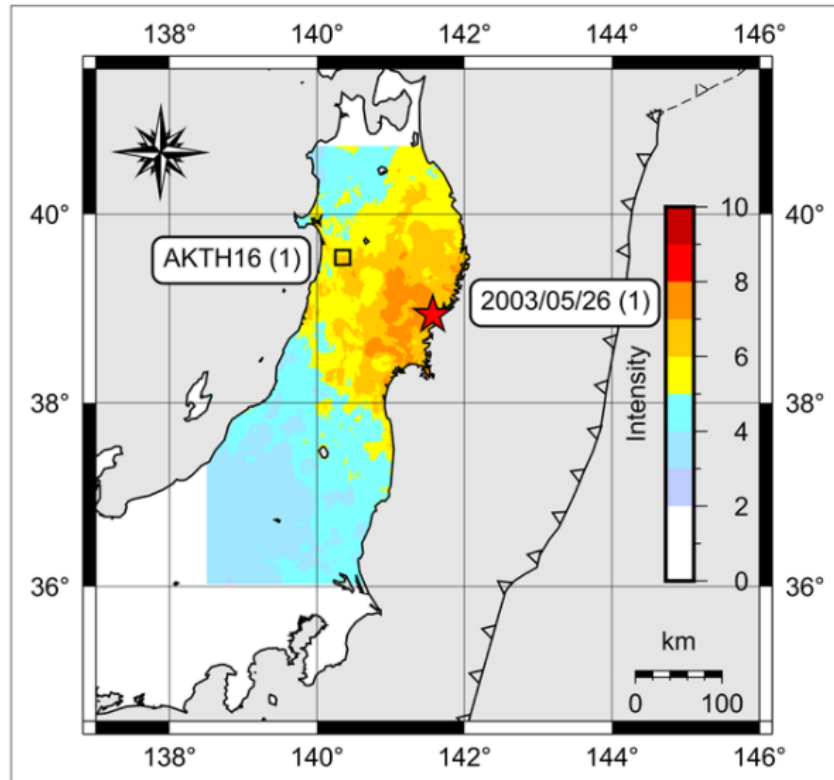
1. HHT-based ERF captures the **earthquake source energy release**, with a **higher resolution** offered by HHT as compared to Fourier analysis methods and wavelet transform.
2. ERF **retains frequency information**, is computationally faster for a rapid interpretation of an event, and **does not entail assumptions** of the fault geometry and velocity structure. These are clear advantages over the traditional MRF.
3. ERF captures **complex ruptures** (2005 Miyagi-Oki event) and sub-events or

OPEN

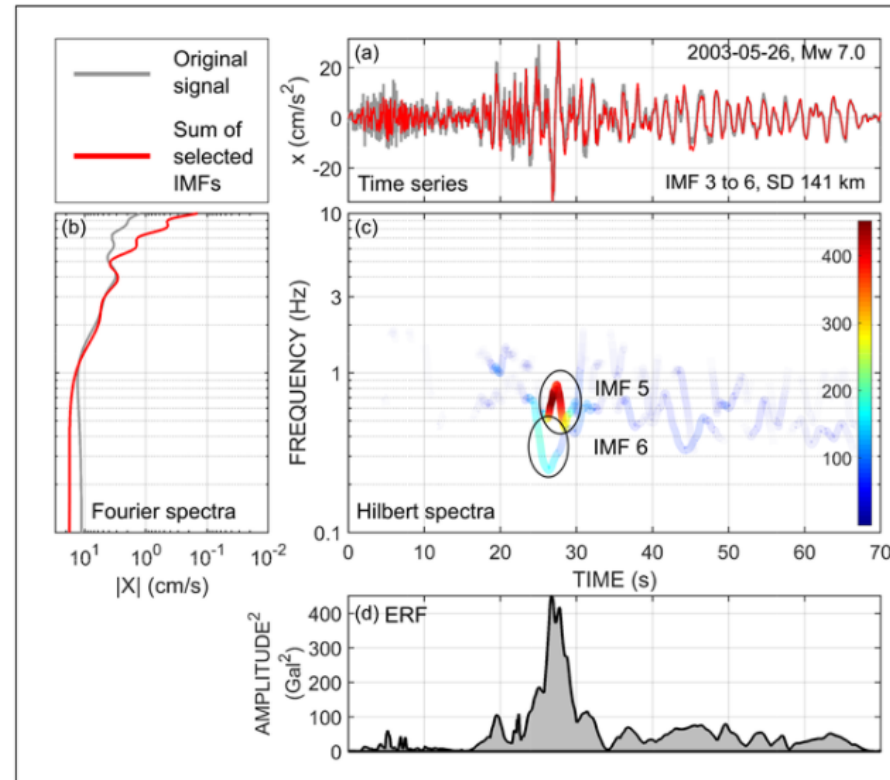
5. Results

1. 26 May 2003 Miyagi Intralab Earthquake (Mw 7.0)

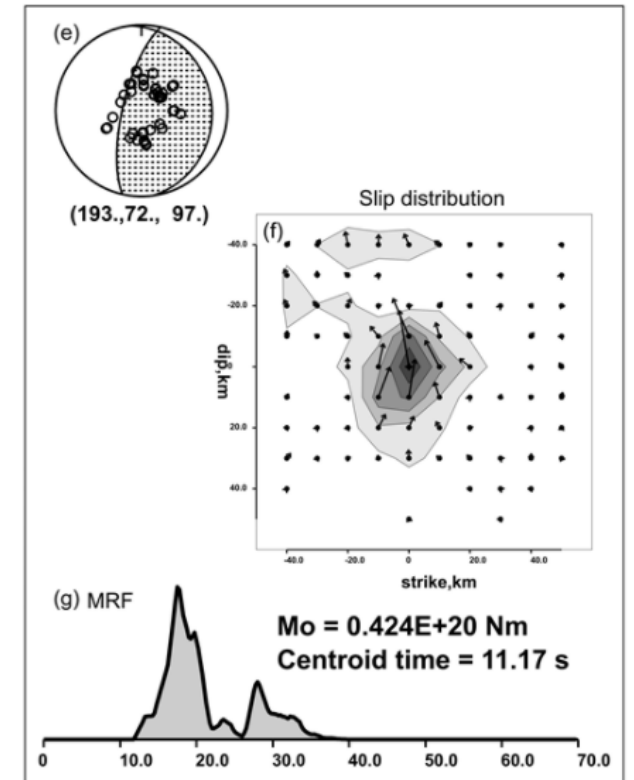
1. 26 May 2003 Miyagi Intralab Earthquake



1.1 Shakemap with epicenter (star) and station (square).



1.2 Strong motion analysis result.

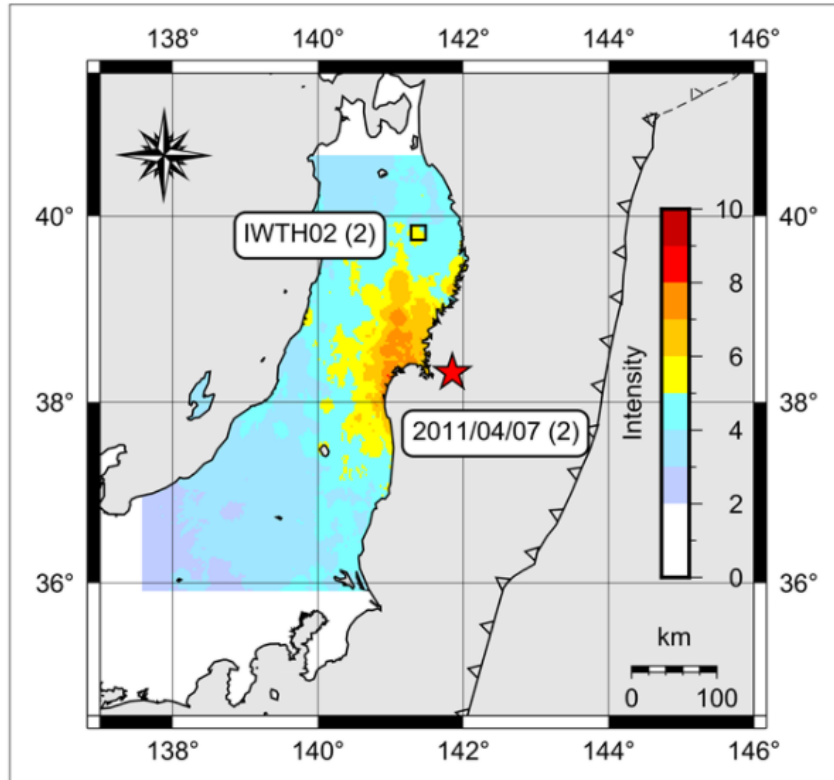


1.3 Teleseismic waveform modeling result.

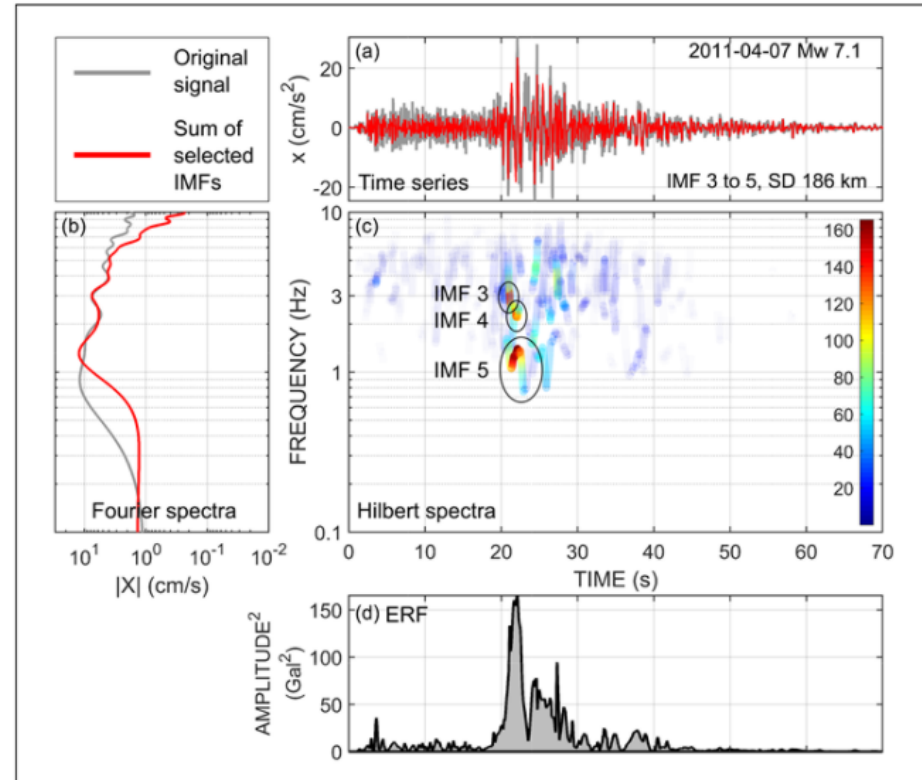
5. Results

1. 26 Mar 2003 Mivagi Intralab Earthquake (Mw 7.0.

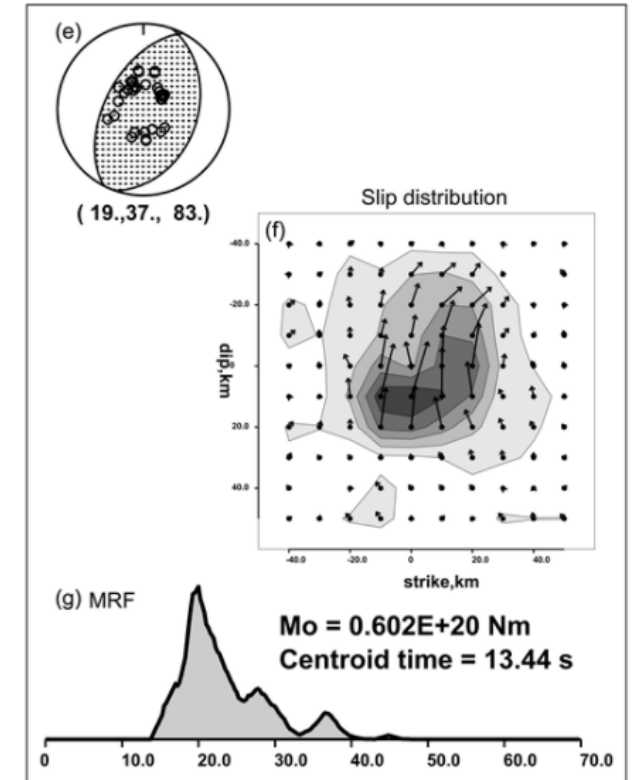
2. 07 April 2011 Miyagi Intralab Earthquake



2.1 Shakemap with epicenter (star) and station (square).



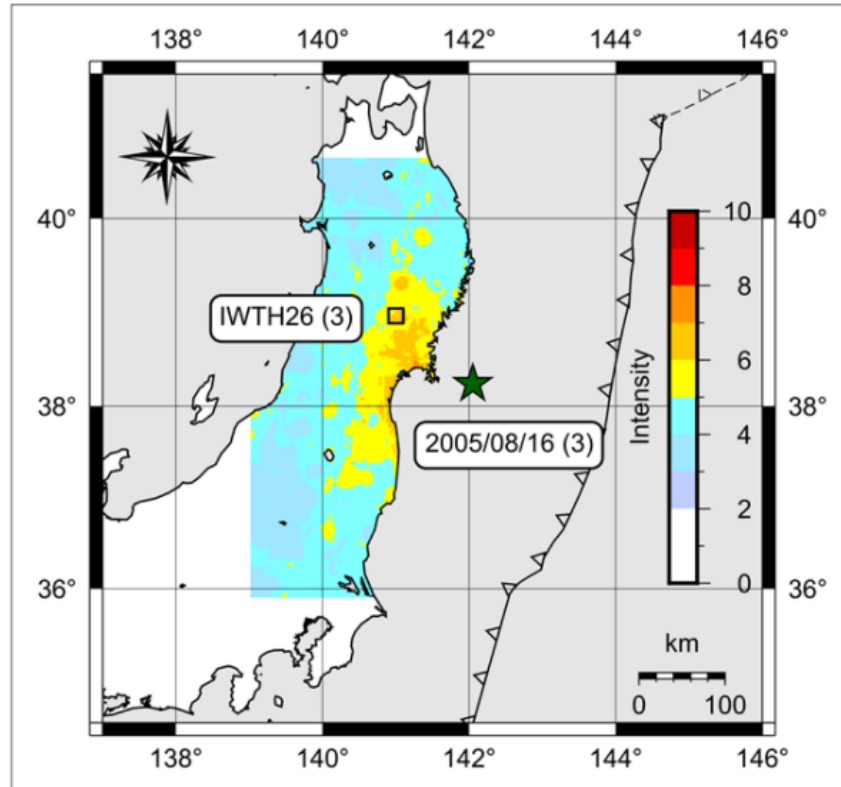
2.2 Strong motion analysis result.



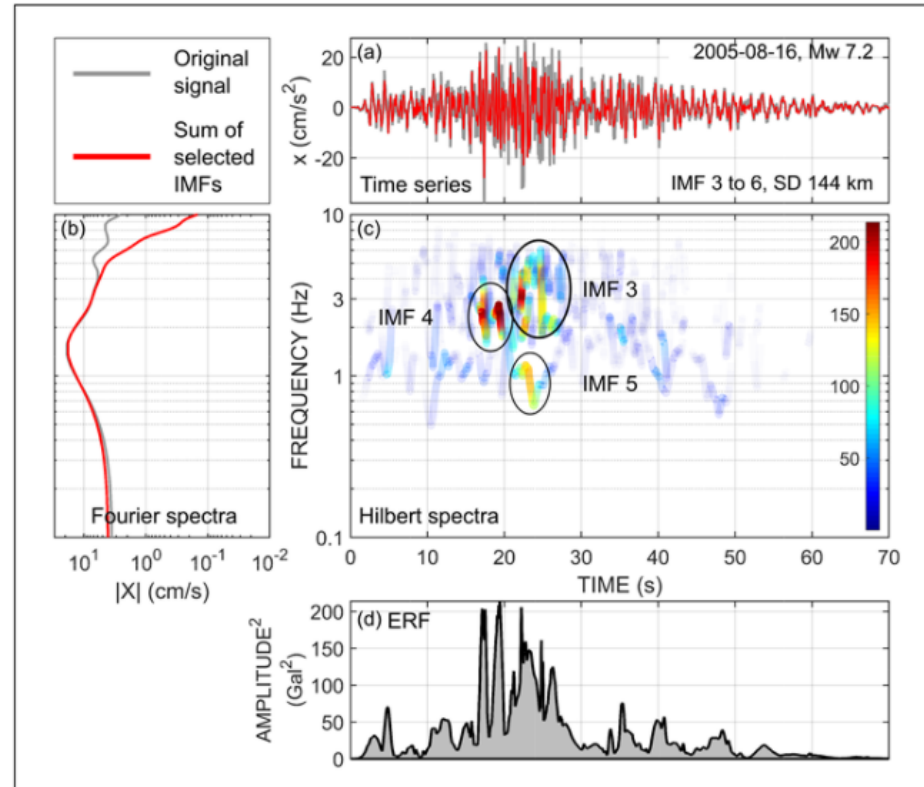
3.3 Teleseismic waveform modeling result.

5. Results

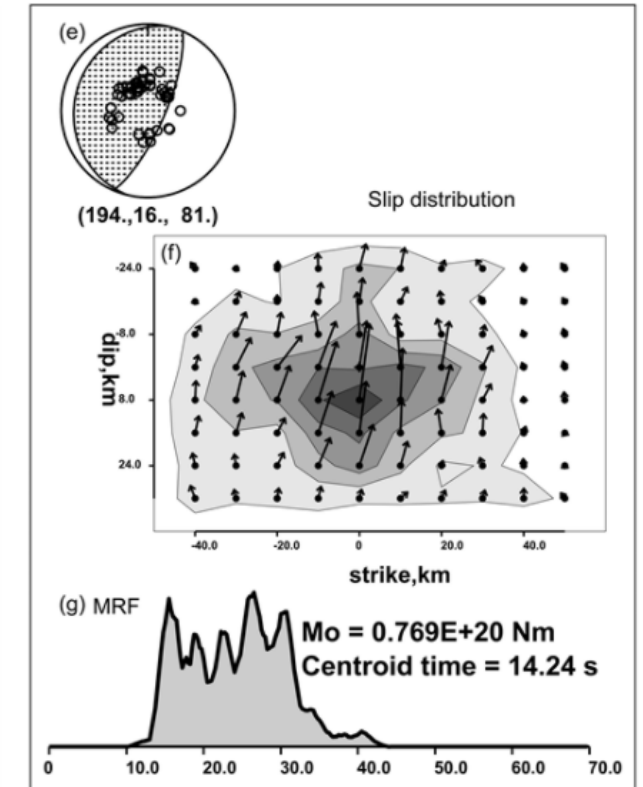
3. 16 August 2005 Miyagi-Oki Interplate Earthquake



3.1 Shakemap with epicenter (star) and station (square).



3.2 Strong motion analysis result.



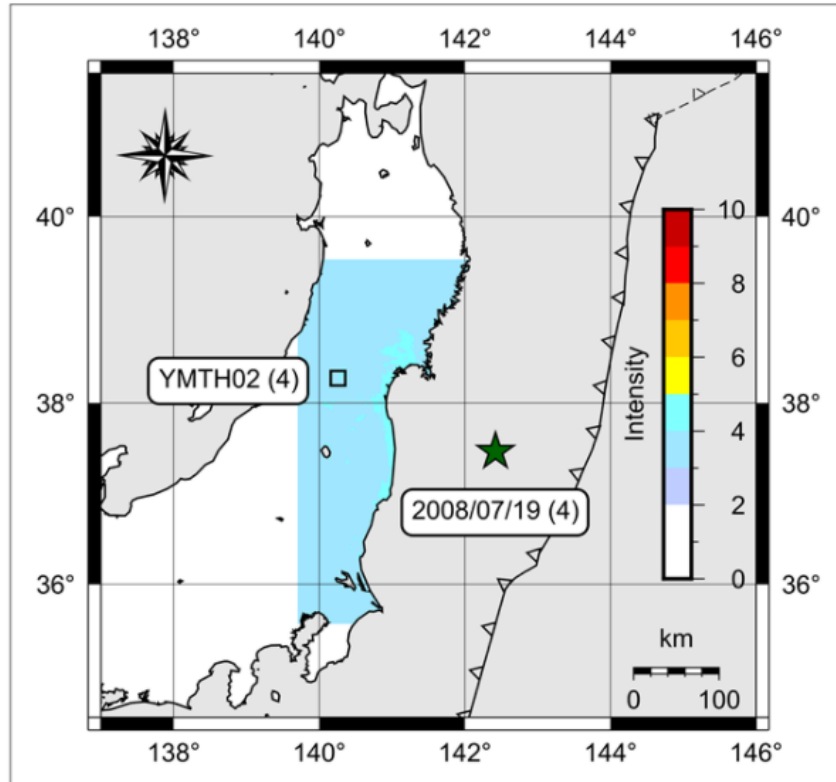
3.3 Teleseismic waveform modeling result.

5. Results

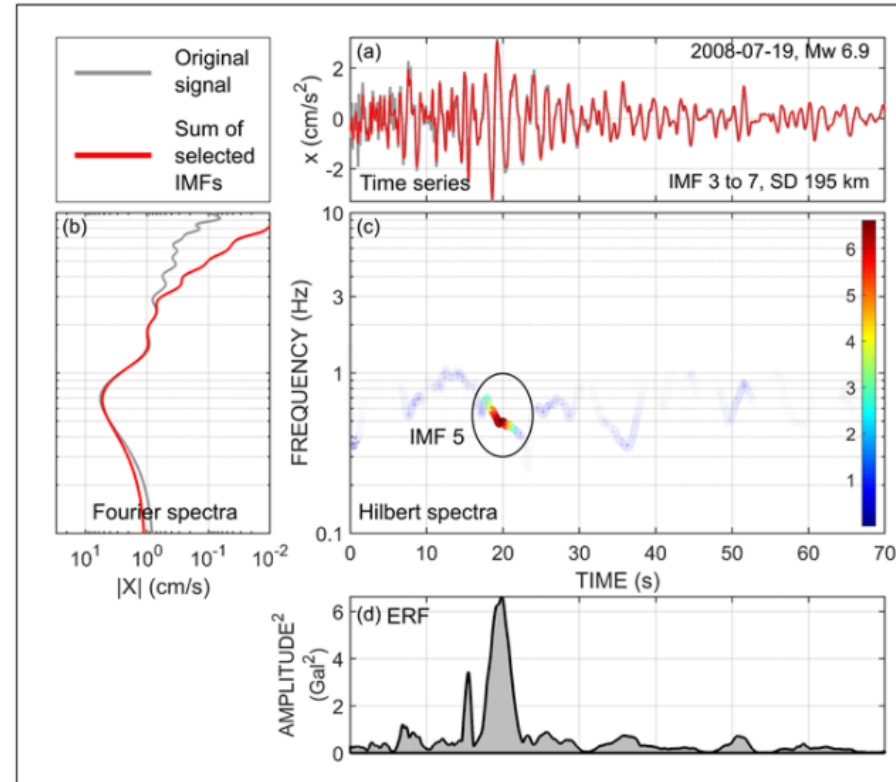
- A shallow interplate event; low-frequency energy

(Ye et al. 2013)

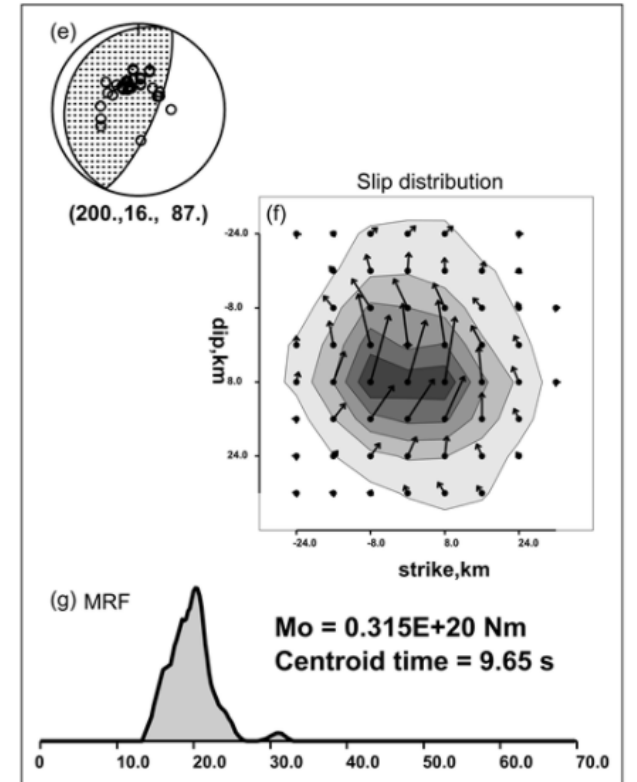
4. 19 July 2008 Fukushima-ken Oki Interplate Earthquake



4.1 Shakemap with epicenter (star) and station (square).



4.2 Strong motion analysis result.



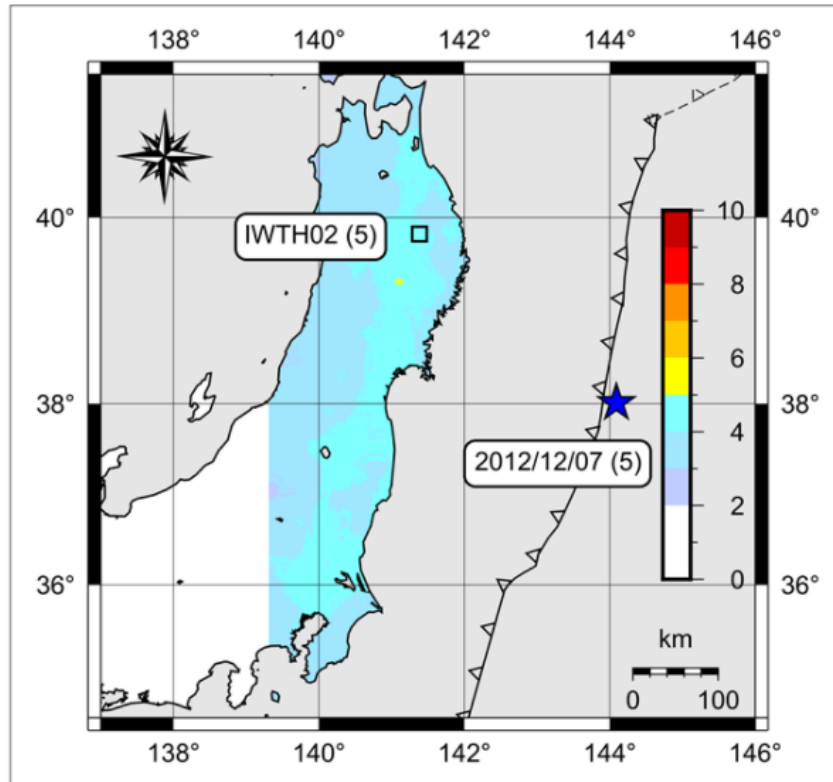
4.3 Teleseismic waveform modeling result.

5. Results

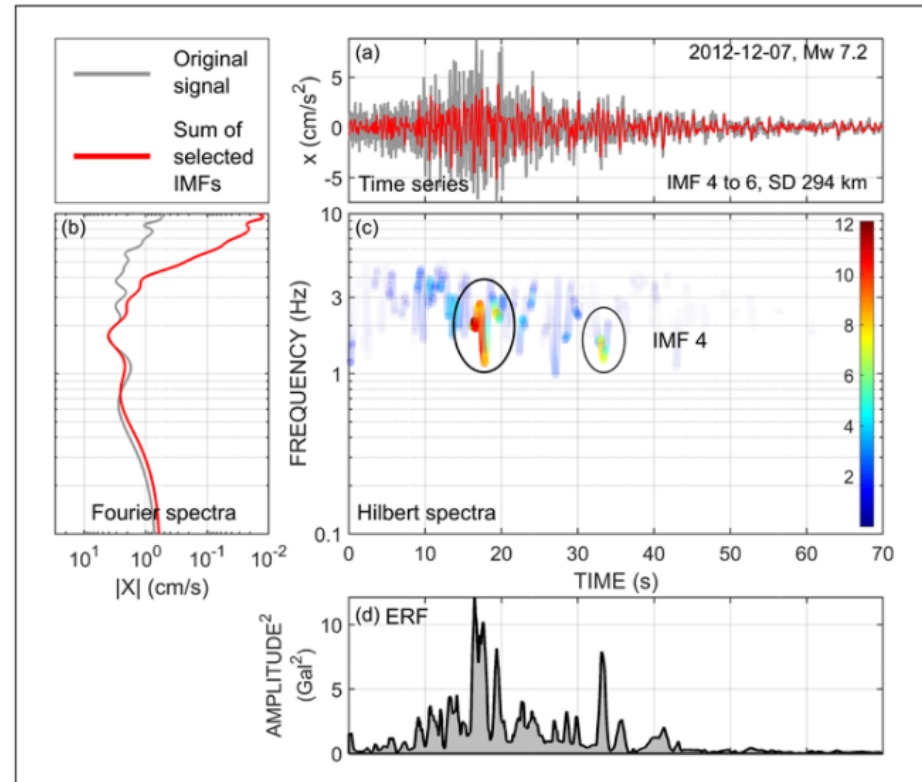
(Ye et al., 2013).

4. 19 July 2008 Fukushima-ken Oki Interplate Earthquake

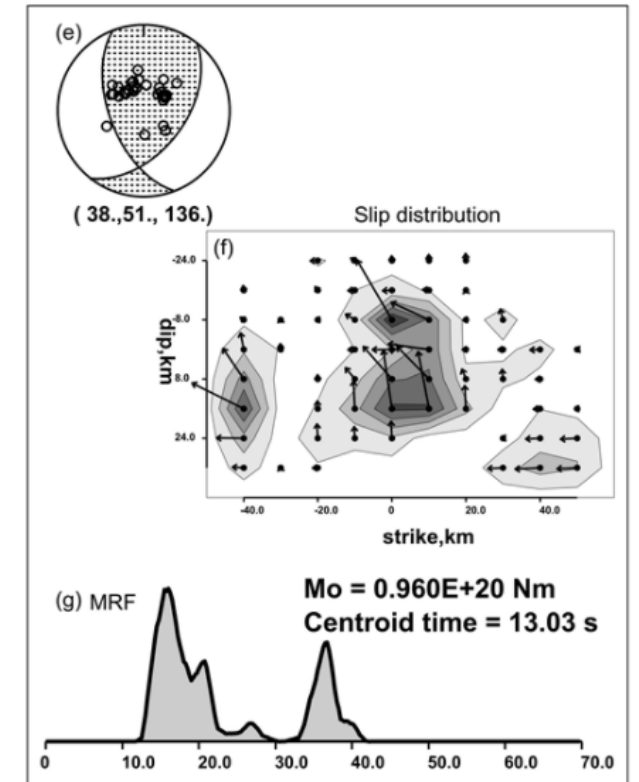
5. 07 December 2012 Kamaishi Intraplate Earthquake



5.1 Shakemap with epicenter (star) and station (square).



5.2 Strong motion analysis result.



5.3 Teleseismic waveform modeling result.

6. Summary

1. HHT-based **ERF captures the earthquake source energy release**, with a **higher resolution** offered by HHT as compared to Fourier analysis methods and wavelet transform.
2. **ERF retains frequency information**, is computationally faster for a rapid interpretation of an event, and **does not entail assumptions** of the fault geometry and velocity structure. These are clear advantages over the traditional MRF.
3. **ERF captures complex ruptures** (2005 Miyagi-Oki event) and sub-events or multiple independent events (2012 Kamaishi event).
4. **Improvement** in the criterion for the **selection of stations** based on their **azimuth**, inferred from the slip distribution. Strike of the Japan Trench provides an important starting point. Further, stations with **seismic intensity** > 3 provide optimal results.
5. **Improvement in the selection of IMF(s)**, based on a **frequency and energy** criterion corresponding with the bandpass filtering in waveform inversion.

1. Key Points

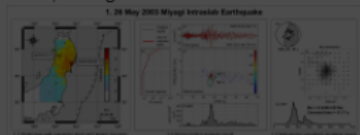
1. Specific Intrinsic Mode Functions (IMFs) represent energy release at the earthquake source.
2. Energy Rate Functions (ERFs) generated from Hilbert spectral analysis of such IMF combinations.
3. Proposed ERFs match well with the Moment Rate Functions (MRFs) from teleseismic waveform modeling.
4. ERF-MRF match is controlled by the station azimuth and shaking intensity, and frequency and energy-based selection of IMFs.

A short video explaining our work

OPEN

5. Results

1. **26 May 2003 Miyagi Intraslab Earthquake (Mw 7.0, depth 67.0 km)**
 - Up-dip slip (towards east-northeast).
 - Station AKTH16, WNW (305.98° azimuth), seismic intensity (SI) 4.
 - Single, dominant, ~10 s energy pulse captured by both the ERF and MRF, along with a weaker tail.



OPEN

4. Methodology

2. Moment Rate Function (MRF) generated from waveform modeling to validate the ERF algorithm.

Selection of strong-motion stations

1. Slip distribution, along with the seismic intensity distribution maps (JMA, 1996; ShakeMap, 2017), used to select stations within the inferred azimuthal range and seismic intensity > 3.



OPEN

6. Summary

1. HHT-based **ERF captures the earthquake source energy release**, with a **higher resolution** offered by HHT as compared to Fourier analysis methods and wavelet transform.
2. **ERF retains frequency information**, is computationally faster for a rapid interpretation of an event, and **does not entail assumptions** of the fault geometry and velocity structure. These are clear advantages over the traditional MRF.
3. **ERF captures complex ruptures** (2005 Miyagi-Oki event) and sub-events or

OPEN